iScience

CellPress
OPEN ACCESS

Article

GPER1 Signaling Initiates Migration of Female V-SVZ-Derived Cells

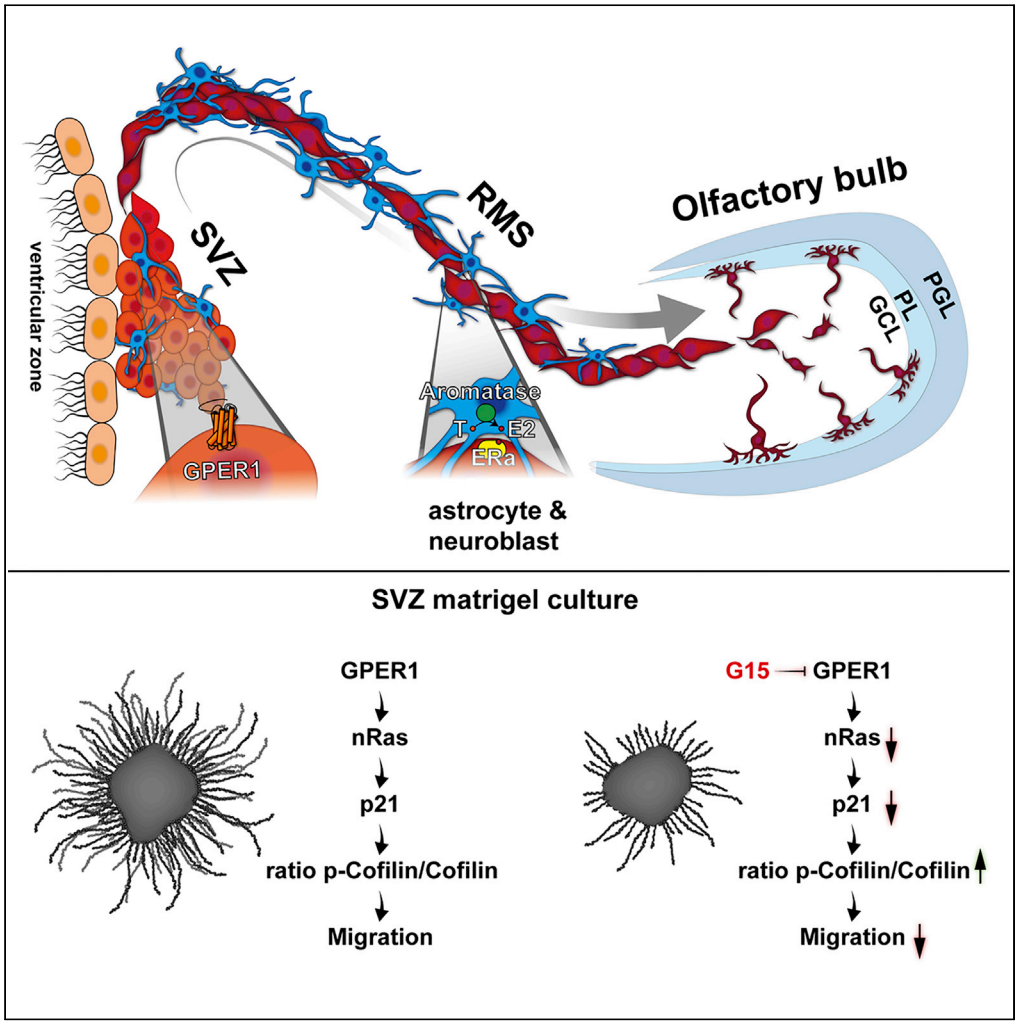

Iris Haumann, Muriel Anne Sturm, Max Anstötz, Gabriele M. Rune

ihaumann@uke.de (I.H.)
rune@uke.de (G.M.R.)

HIGHLIGHTS

GPER1 is expressed within all cell types of the stem cell lineage in the V-SVZ

Blocking of GPER1 leads to a decrease in migration of V-SVZ-derived neuroblasts

GPER1 signaling in V-SVZ Matrigel cultures involves Ras-induced p21

Blocking of GPER1 signaling leads to an increase in the ratio of p-cofilin/cofilin

Haumann et al., iScience *23*, 101077
May 22, 2020
https://doi.org/10.1016/j.isci.2020.101077

iScience

CellPress
OPEN ACCESS

Article

GPER1 Signaling Initiates Migration of Female V-SVZ-Derived Cells

Iris Haumann,[1,*] Muriel Anne Sturm,[1] Max Anstötz,[1] and Gabriele M. Rune[1,2,*]

SUMMARY

In the rodent ventricular-subventricular zone (V-SVZ) neurons are generated throughout life. They migrate along the rostral migratory stream (RMS) into the olfactory bulb before their final differentiation into interneurons and integration into local circuits. Estrogen receptors (ERs) are steroid hormone receptors with important functions in neurogenesis and synaptic plasticity. In this study, we show that the ER GPER1 is expressed in subsets of cells within the V-SVZ of female animals and provide evidence for a potential local estrogen source from aromatase-positive astrocytes surrounding the RMS. Blocking of GPER1 in Matrigel cultures of female animals significantly impairs migration of V-SVZ-derived cells. This outgrowth is accompanied by regulation of phosphorylation of the actin-binding protein cofilin by GPER1 signaling including an involvement of the p21-Ras pathway. Our results point to a prominent role of GPER1 in the initiation of neuronal migration from the V-SVZ to the olfactory bulb.

INTRODUCTION

In the rodent brain, the ventricular-subventricular zone (V-SVZ) is located along the walls of the brain lateral ventricles and new neurons are continuously generated throughout life (Apple et al., 2017; Doetsch et al., 1997; Ponti et al., 2013a, 2013b). A monolayer of ependymal cells lines the ventricle, and adjacent located neural stem cells (type B cells) undergo self-renewal before differentiating into intermediate rapidly dividing progenitors (type C cells), which then give rise to neuroblasts (type A cells) (Luskin, 1993; Lois and Alvarez-Buylla, 1994). These neuroblasts, in turn, migrate in chains rostrally along the RMS into the olfactory bulb (OB). Here, they switch from tangential to radial migration to reach their final destination within the OB and differentiate into functional interneurons.

Newly generated OB interneurons play an important role in the formation and maintenance of olfactory circuits, and as a consequence control important behaviors such as social recognition, reproductive behavior (e.g., mate selection), and parental care (Marrocco and McEwen, 2016; McEwen and Milner, 2017; Shingo et al., 2003; Larsen et al., 2008; Larsen and Grattan, 2010; Mak and Weiss, 2010). Although sex hormones play a key role in the regulation of these behaviors (Young, 1961; Young et al., 1964; Lisk and Suydam, 1967; Davis et al., 1979; Pfaff, 1980; Mak et al., 2007), only few studies have focused on the role of gonadal hormones and their receptors in neurogenesis in the V-SVZ, and subsequently in the regulation of olfactory circuits (Mouret et al., 2009; Brock et al., 2010). For hippocampal neurogenesis it has been shown that steroids such as estrogens play a key role both during development and in adulthood (Tanapat et al., 1999; Banasr et al., 2001; Fester et al., 2006). Studies that have addressed potential effects of estradiol (E2) on proliferation of cells in the rodent V-SVZ have reported that E2 increases the number of embryonic but not adult neural stem cells (Brännvall et al., 2002; Veyrac and Bakker, 2011; Martínez-Cerdeño et al., 2006). This holds true for rats and mice. Other experiments, in contrast, point to prolactin as being an essential player in stimulating neurogenesis in the V-SVZ (Shingo et al., 2003; Lennington et al., 2003).

Potential E2 effects on olfactory neurogenesis and migration of neuroblasts from the V-SVZ to the OB would require estrogen receptors (ER). E2 classically signals via the two ERs, ERα and ERβ, which belong to the superfamily of nuclear steroid hormone receptors. These receptors function as hormone-inducible transcription factors and upon binding of E2 induce gene transactivation. It has been previously shown that ERα, but not ERβ, mRNA is expressed within the V-SVZ (Isgor and Watson, 2005). In contrast, within the OB of rats and mice, both ERs and aromatase, the enzyme that converts testosterone into estradiol, have been found to be expressed (Hoyk et al., 2006, 2014; Horvath and Wikler, 1999; Veyrac and Bakker, 2011).

[1]Institute of Neuroanatomy, University Medical Center Hamburg-Eppendorf (UKE), Hamburg, Germany

[2]Lead Contact

*Correspondence: ihaumann@uke.de (I.H.), rune@uke.de (G.M.R.)

https://doi.org/10.1016/j.isci.2020.101077

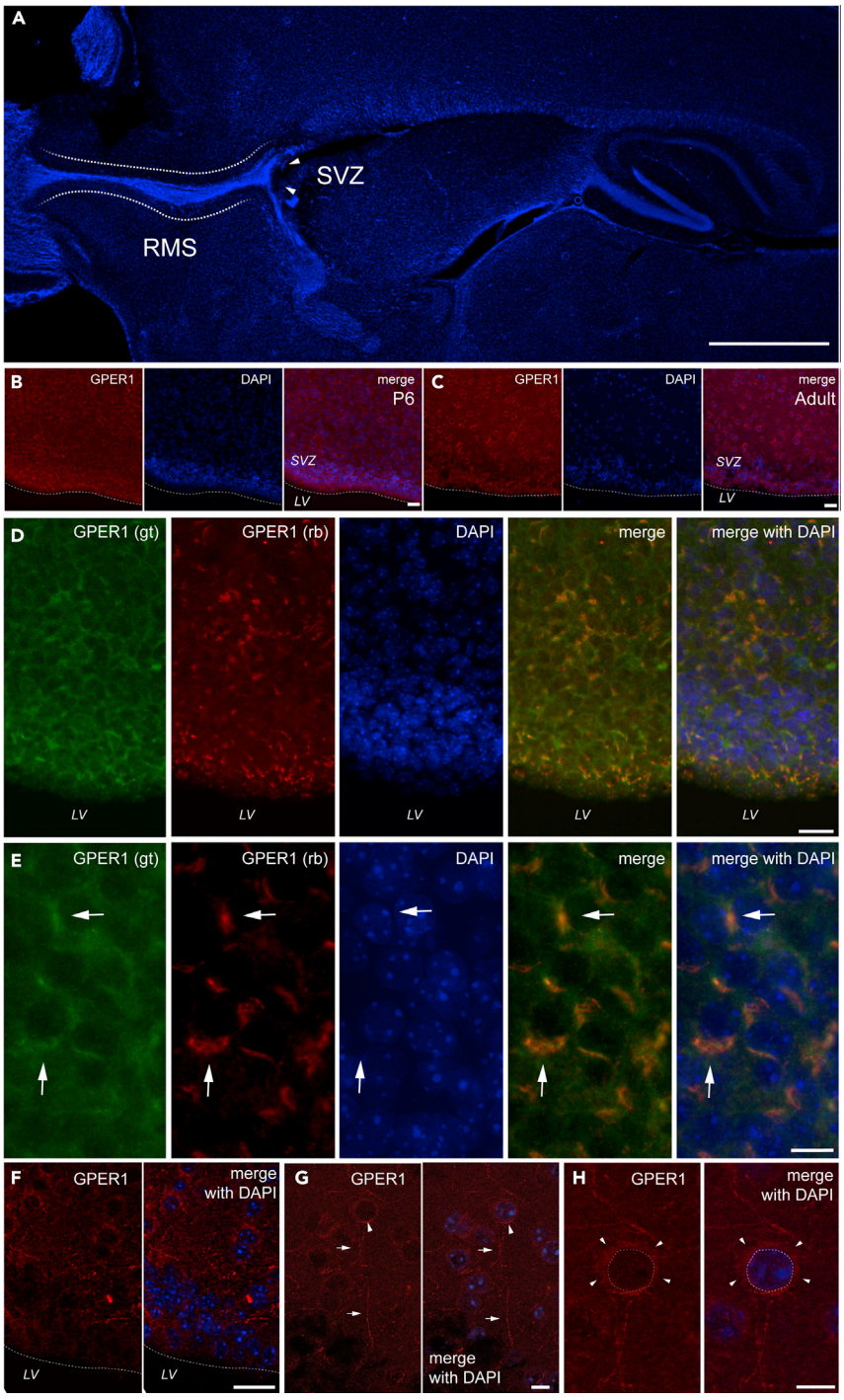

Figure 1. GPER1 is Expressed in the Postnatal and Adult V-SVZ

(A) Low-magnification fluorescence image with DAPI labeling, showing the SVZ (arrowheads) and the RMS (dotted lines) in a sagittal vibratome section of an adult female mouse brain.

(B) Low-magnification confocal image of GPER1 (rb) expression in a P6 female brain section. GPER1 is expressed already at P6 in the neurogenic niche. The dotted line represents the border separating the lateral ventricle from the V-SVZ area.

(C) Low-magnification images of 7-μm-thick paraffin sections of an adult female mouse brain, showing GPER1 (rb) expression in the V-SVZ next to the lateral ventricle. The dotted line represents the border separating the ventricle from the V-SVZ area.

Figure 1. *Continued*

(D) Low-magnification pictures of rabbit- and goat-derived antibody immunohistochemistry of GPER1 taken from adult female mouse brain vibratome sections. Note that both antibodies label the same population of cells, although the staining intensity differs slightly.

(E) High-magnification image of GPER1 (rb and gt)-positive cells from adult female V-SVZ showing colabeling of both antibodies. Of note immunoreactivity is mostly restricted (highest intensity) to one side of the cell (arrows).

(F) Low-magnification fluorescence image showing GPER1 expression in the V-SVZ. (G) Higher magnification shows that in some cases, GPER immunohistochemistry revealed labeled processes of cells (arrows). (G and higher-magnification image in H) GPER1 expression is also seen in the cytoplasm surrounding (marked by arrowheads) the nucleus. LV, lateral ventricle; RMS, rostral migratory stream; SVZ, subventricular zone; gt, goat antibody; rb, rabbit antibody. Scale bars: 500 μm in (A), 10 μm in (D), 5 μm in (E), 20 μm in (F), and 5 μm in (G and H).

In addition to the transcription factors ERα and ERβ, a G protein-coupled receptor (GPCR)-30 (GPR30) was shown to mediate rapid or "pregenomic" effects of estrogen, events that occur within minutes after ligand exposure. The receptor was therefore named *G protein-coupled ER* (GPER)-1 (Filardo et al., 2002; Revankar et al., 2005; Thomas et al., 2005). GPER1 has a high affinity to estrogens and is localized either in the plasma membrane or in the endoplasmic reticulum (Prossnitz et al., 2008). To date no information is available for a possible role of GPER1 signaling in the V-SVZ in respect to E2 functions. In this study, we therefore analyzed the expression of GPER1 and ERα and show that GPER1 is expressed in specific cells of the V-SVZ of adult and P6 female mice. To be on the safe side, we used female animals only, as with respect to synaptic plasticity, estrogenic effects in the brain have frequently been shown to differ in the hippocampus of males and females (Brandt et al., 2019; Brandt and Rune, 2019; Vierk et al., 2012). In this study, we provide evidence for a role of GPER1 in the control of neuroblast migration. Moreover, we identify Ras-mediated signaling mechanisms and p21-dependent modulation of cofilin as being crucial in GPER1-mediated regulation of neuroblast migration.

RESULTS

To date our knowledge on the role of ERs in the modulation of processes within the V-SVZ is still elusive. In particular, nothing is known about the expression and localization of the recently described GPER1 in the V-SVZ and the adjacent RMS. Therefore, we analyzed the expression of GPER1, using fluorescence-based immunohistochemical analysis to detect the ER expression in adult female brains and in particular in brains of female P6 animals. We also analyzed ERα, whose mRNA in contrast to that of ERβ was found in the V-SVZ. The immunohistochemical data of the P6 animals were compared with data from Matrigel cultures, which were generated on P4-P5 and cultivated for 24 h.

Cell-Specific GPER1 Expression in the V-SVZ of Early Postnatal and Adult Mice

In the case of GPER1 we took advantage of a polyclonal antiserum generated in rabbit, which was raised against a synthetic C-terminal peptide of GPER1 and that has previously been used for immunohistochemistry in various tissues including mouse brain tissue (Bondar et al., 2009; Du et al., 2012; Samartzis et al., 2014; Li et al., 2019; Wang et al., 2018; Wu et al., 2018; Kanageswaran et al., 2016). The specificity of the antibody has been verified in different independent studies including controls in a GPER-negative cell line and in shGPER-1 knockdown tissue (Du et al., 2012; Samartzis et al., 2014; Li et al., 2019). Another antibody raised in goat that is also directed against a synthetic C-terminal peptide of GPER1 was used for control purposes. GPER1 was previously described to be localized at the membrane and/or in the cytoplasm, where its localization was postulated to be restricted to the endoplasmic reticulum (Revankar et al., 2005; Funakoshi et al., 2006; for review see Filardo and Thomas, 2012). Importantly, upon ligand binding, the receptor is internalized before degradation, which may explain that the receptor is commonly detected intracellularly (Cheng et al., 2011). In cells of the V-SVZ of early postnatal mice and in cells of adult mice GPER1 was abundantly expressed (Figures 1A–1C and S1A). Colabeling of the two GPER1 antibodies revealed an identical labeling pattern, which underscores the specificity of our antibodies (Figures 1D and 1E). On the cellular level, we found GPER1 immunoreactivity surrounding the cell bodies and also occasionally in cellular processes (cell bodies: Figure 1E; arrowhead in Figures 1G and 1H; processes: Figures 1F and arrows in 1G). Interestingly, in many cases a clear asymmetric distribution of immunoreactivity was seen in GPER1-positive cells, with stronger labeling on one side of the cell body (arrows in Figure 1E).

The expression of GPER1 in many, but not all, cells of the V-SVZ tempted us to define the cell type in the stem cell niche that expresses GPER1. The lineage of cells within the V-SVZ comprises type B1 and B2

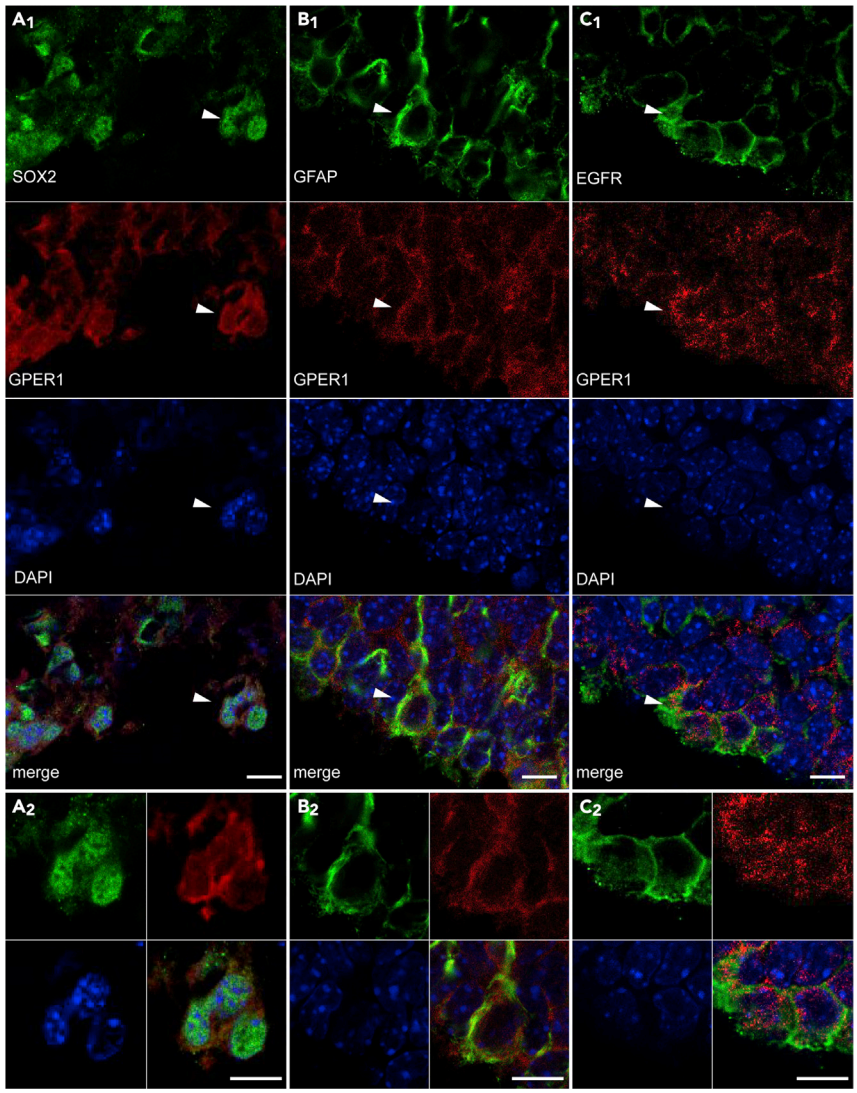

Figure 2. GPER1 is Expressed by Different Cell Types in the V-SVZ of Early Postnatal Mice

Confocal images of 7-μm-thick paraffin sections showing double immunofluorescence in the V-SVZ of P6 female mice to demonstrate expression of GPER1 in different cell types within the stem cell niche. (A_1) SOX2 is used as a marker for type B and type C cells. Merged image illustrates colabeling of SOX2 (rb) and GPER1 (gt). (A_2) Higher magnification showing GPER1 immunoreactivity surrounding nuclear labeling of SOX2. (B_1) Type B cells, identified by their expression of GFAP, also express GPER1. Merged images and higher-power magnification in (B_2) reveal cells coexpressing GFAP (rb) and GPER1 (gt). (C_1 and higher-magnification image in C_2) GPER1 (gt) is also expressed in EGFR-positive type C cells (rb). All arrows point to cells displaying colocalization. gt, goat antibody; rb, rabbit antibody. Scale bars, 10 μm.

astrocytes, transient amplifying progenitor cells (type C cells), and neuroblasts (type A cells) (Doetsch et al., 1997; Fuentealba et al., 2012).

Type B and type C cells are visualized by their expression of the transcription factor SOX2 (Mamber et al., 2013), and we found many GPER1/SOX2 double-positive cells in P6, as well as in adult animals (Figures 2A and 3A). To identify whether GPER1 is expressed in type B cells we performed double-labeling using anti-GFAP and anti-Vimentin, both being markers of type B astrocytes (Mamber et al., 2013). Both markers are expressed in P6 and adult animals. We found GPER1/GFAP-positive (Figure 2B) as well as GPER1/Vimentin-positive cells (Figure 3B), which demonstrates that GPER1 is indeed expressed in type B cells in P6 and adult animals. A few cells expressed GPER1 but did not show labeling of GFAP or Vimentin (see arrowheads in Figure 3B). To test whether these cells represent type C cells, we used an antibody against epidermal

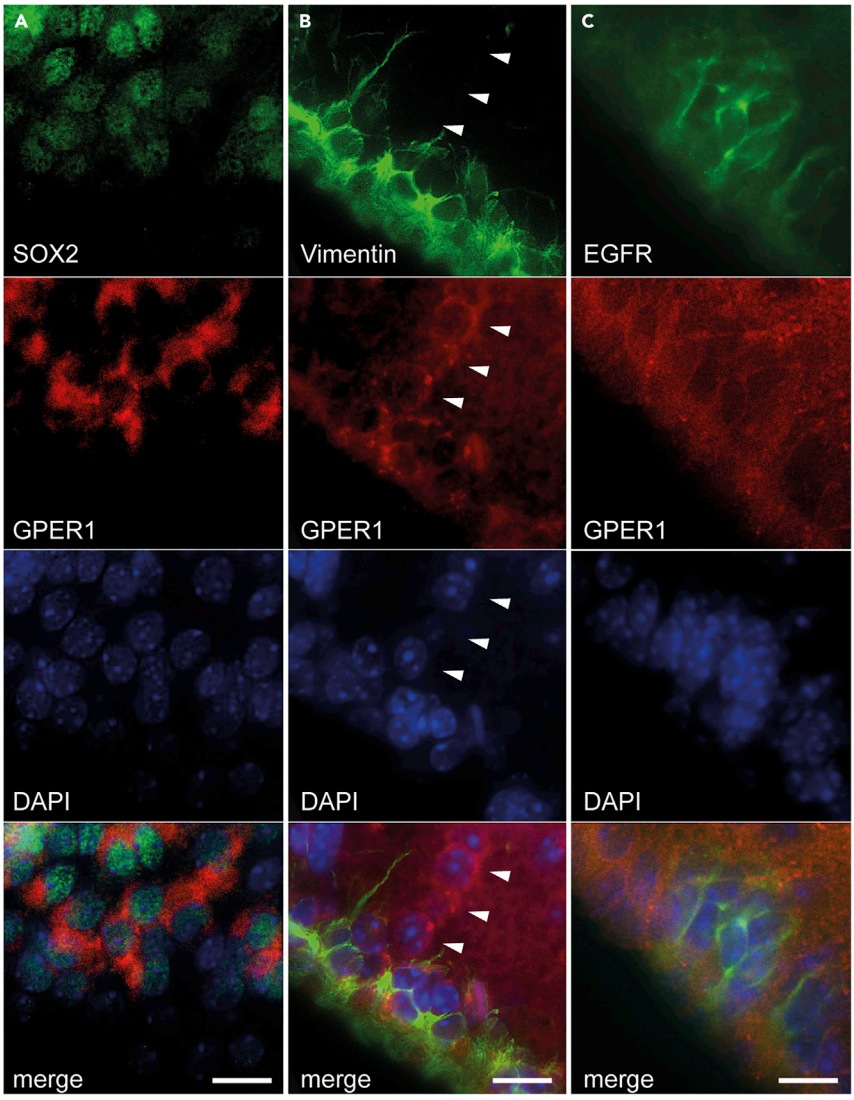

Figure 3. GPER1 is Expressed by Different Cell Types in the V-SVZ of Adult Mice

Fluorescence images of 7-μm-thick paraffin sections showing double immunofluorescence in the V-SVZ of adult female mice to demonstrate expression of GPER1 in the different cell types of the stem cell niche.

(A) As in P6 animals, GPER1 immunohistochemistry (gt) in adult animals shows colabeling with SOX2 (rb) as a marker for type B and type C cells.

(B) GPER1 (gt) also colocalizes with Vimentin (rb), a marker for type B cells. Note that not every cell expressing GPER1 is also positive for Vimentin (see arrowheads).

(C) GPER1 (gt) shows weak coexpression with EGFR (rb), a marker for type C cells. Merged images illustrate colocalization. gt, goat antibody; rb, rabbit antibody. Scale bars, 20 μm.

growth factor receptor, a marker of transiently dividing C cells (Mamber et al., 2013). We found co-expression of GPER1 and EGFR in some cells of P6 animals (Figure 2C), whereas only very few and very weakly stained cells were seen in the adult stem cell niche (Figure 3C).

The microtubule-associated protein Doublecortin (DCX) is an established marker for type A neuroblasts (Mamber et al., 2013). Double-labeling with antibodies against DCX and GPER1 revealed that in P6 animals GPER1-positive cells were occasionally also positive of DCX and thus identified as type A neuroblasts (Figures 4A and 4B). Apart from a small area at the beginning of the RMS, the neuroblasts in the RMS were devoid of any GPER1 immunolabeling (Figure 4C).

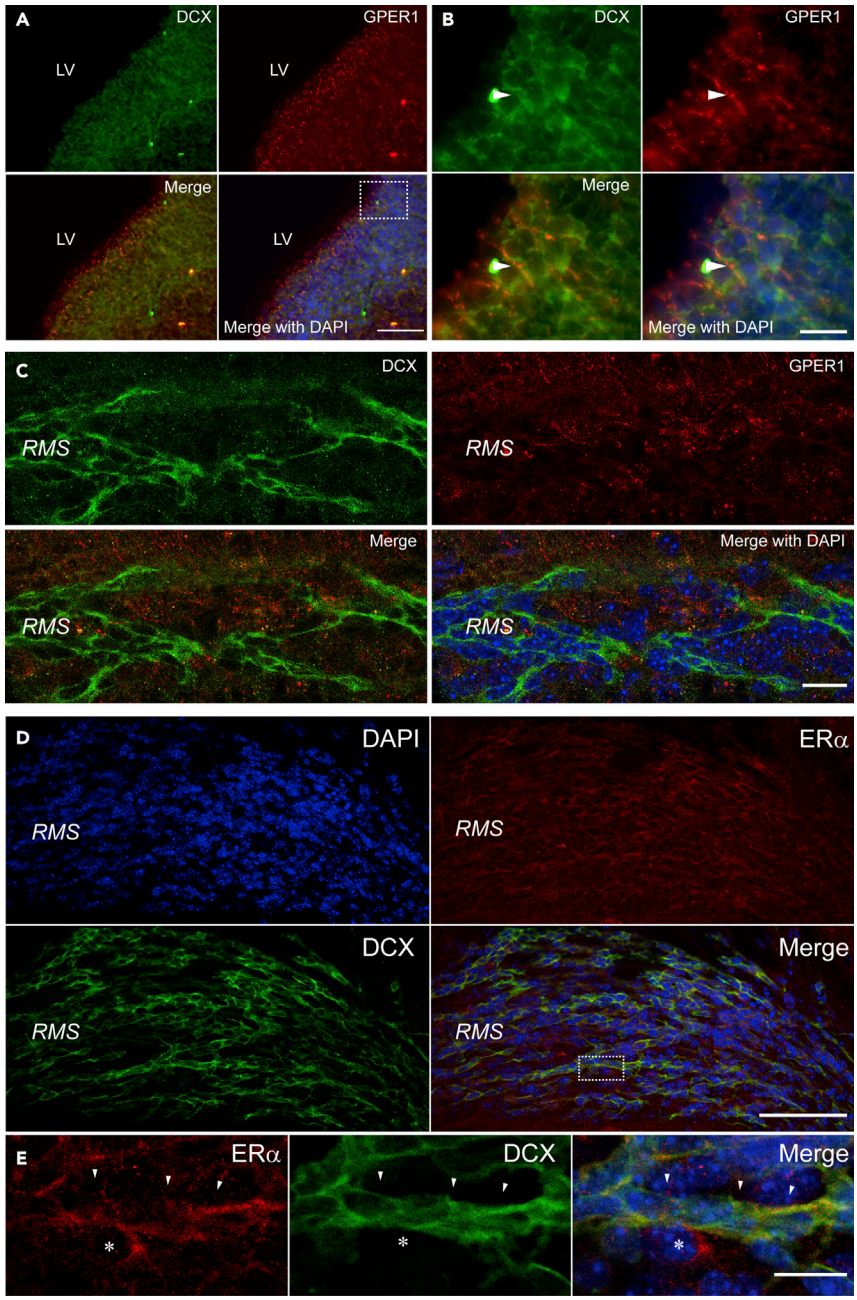

Figure 4. GPER1 and ERα Show a Different Expression Pattern in DCX-Positive Neuroblasts

(A and higher-magnification image in B) Fluorescence images of 7-μm-thick paraffin sections showing double immunofluorescence in the V-SVZ of P6 female mice to demonstrate colocalization of GPER1 (rb) with DCX (gt) in type A neuroblasts. The higher magnifications show that GPER1 is expressed in DCX-positive cells in the V-SVZ. The arrowheads point to cells displaying colocalization. Note that GPER1 often shows a polarized distribution at the cell membrane (arrowheads).

(C) Double immunofluorescence confocal images showing GPER1 (rb) and DCX (gt) in the RMS of an adult female mouse, taken from 50-μm-thick vibratome sections. Note that although GPER1 and DCX immunoreactivity is closely associated, DCX-expressing cells are not positive for GPER1.

(D and higher-magnification image in E) Confocal images showing immunofluorescence with DCX (gt) and ERα (rb) in the RMS. Higher magnification demonstrating that ERα is expressed by DCX-positive neuroblasts. Arrowheads point to cells showing co-immunoreactivity. Few cells in the RMS express ERα but are negative for DCX (asterisks). LV, lateral ventricle; RMS, rostral migratory stream.

Scale bars: 50 μm in (A), 10 μm in (B), 15 μm in (C), 50 μm in (D) and 10 μm in (E).

As a result, we found GPER1 to be expressed by subsets of all cell types of the stem cell lineage (type B, type C, and type A cells) in the V-SVZ. It needs to be mentioned that not every cell expressing one of the marker molecules was also positive of GPER1, suggesting that only a subset of each cell type expresses the receptor. Importantly, whereas immunoreactivity of GPER1 was abundant in the V-SVZ, immunoreactivity of GPER1 was missing in type A cells in the RMS.

Estrogen Receptor ERα Expression in the V-SVZ and the RMS

In addition to the expression of GPER1, we analyzed the localization of the classical genomic ERα in the V-SVZ and the RMS in adult and postnatal mice using immunohistochemistry. The specificity of the antibody was controlled by preadsorption with the immunizing peptide (see Figure S1D and S1E). In earlier studies, it was shown that ERα is not only localized in the cytoplasm and/or in the nucleus (Jensen and DeSombre, 1973; Arnal et al., 2017) but also in the plasma membrane (Pappas et al., 1995; Marino et al., 2006; Pedram et al., 2014; Razandi et al., 1999). In accordance with these previous descriptions, we found ERα immunoreactivity subcellularly localized in the cytoplasm/nucleus (higher magnification in Figure S1D) and additionally within the plasma membrane (Figures 4D and 4E). ERα-positive cells were ubiquitously present within the V-SVZ and in the RMS of adult (Figures S1B and S1D, and Figures 4D and 4E) and P6 animals (Figure S1C). Using co-immunohistochemistry with anti-DCX and anti-ERα, we found that ERα is present in migrating type A cells of the RMS (arrowheads in Figure 4E).

The strong expression of ERα in DCX-positive cells within the RMS together with strong abundance of the receptor in the V-SVZ, but the lack of GPER1 expression in neuroblasts of the RMS, indicates that estrogenic signaling in cells of the neurogenic niche differs from estrogenic signaling in the RMS.

Aromatase Is Expressed within the V-SVZ and in the RMS

In the last years it has become increasingly evident that locally synthesized estradiol rather than estradiol from peripheral sources influences cerebral function, for instance, neuronal migration, synaptogenesis, and axon outgrowth (Williams et al., 1999; Wang et al., 2003; Kretz et al., 2004; Rune and Frotscher, 2005; Prange-Kiel and Rune, 2006; Prange-Kiel et al., 2006; von Schassen et al., 2006). In an attempt to identify a potential source of estradiol for the estrogen receptors in the neurogenic niche and the RMS we analyzed the expression of aromatase, the final enzyme of the estradiol synthesis.

The specificity of the aromatase antibody was controlled by preadsorption with the immunizing peptide (Figure S2A–S2C). We found strong expression of aromatase in the stem cell niche (Figure 5A) and within the RMS (Figures 5B and 5C). This was the case in adult and P6 animals (data not shown) as well. Performing triple labeling of aromatase, DCX (to label migrating type A neuroblasts), and GFAP (to label astrocytes), we observed no co-labeling of aromatase and migrating DCX-positive neuroblasts (Figures 5B and 5C). In contrast, we found colocalization of aromatase and GFAP in astrocytes surrounding the migrating neuroblasts (Figure 5B and higher magnification in Figure 5C). To further substantiate our finding that glial cells express aromatase we used S100β, another marker for astrocytes, and we also observed co-expression of GFAP and S100β (Figure 5D). This finding strongly suggested that astrocytes, forming the well-known tube-like structure that surrounds the migrating neuroblasts, might be a source of estradiol. Thus, astrocytes in the neurogenic niche and the RMS may provide the ligand for ER-mediated functions during migration.

Blocking of GPER1 with G15 Resulted in Reduced Cellular Migration of V-SVZ-Derived Matrigel Explants

Upon our finding of abundant expression of GPER1 in cells of the V-SVZ and our findings that astrocytes of the V-SVZ and of the RMS are aromatase-positive cells and may serve as a local source of estrogens, we hypothesized that GPER1 is involved in starting migration of cells from the V-SVZ. To test this hypothesis, we performed Matrigel explant cultures of V-SVZ tissue and analyzed the migration of cells in the presence of the GPER1 signaling antagonist G15 (Dennis et al., 2009). We cultured the explants for 24 h in the presence or absence of G15 and monitored their migration. The analysis of migratory outgrowth from the explants was performed following the method of Dixon et al. (Dixon et al., 2017). Accordingly, we performed a semi-quantitative classification, ranking the explants into four grades depending on the number of chains outgrown from the explant: grade1 (less than 10 chains), grade 2 (10–50 chains), grade 3 (50–100 chains), and grade 4 (more than 100 chains) (see Figure 6A). All explants with chains were considered for analysis. In total, we analyzed 197 explants (control: n = 100; G15: n = 97) from 18 animals. It is of note in this context that every animal delivers explants that were either treated with G15 or taken as controls,

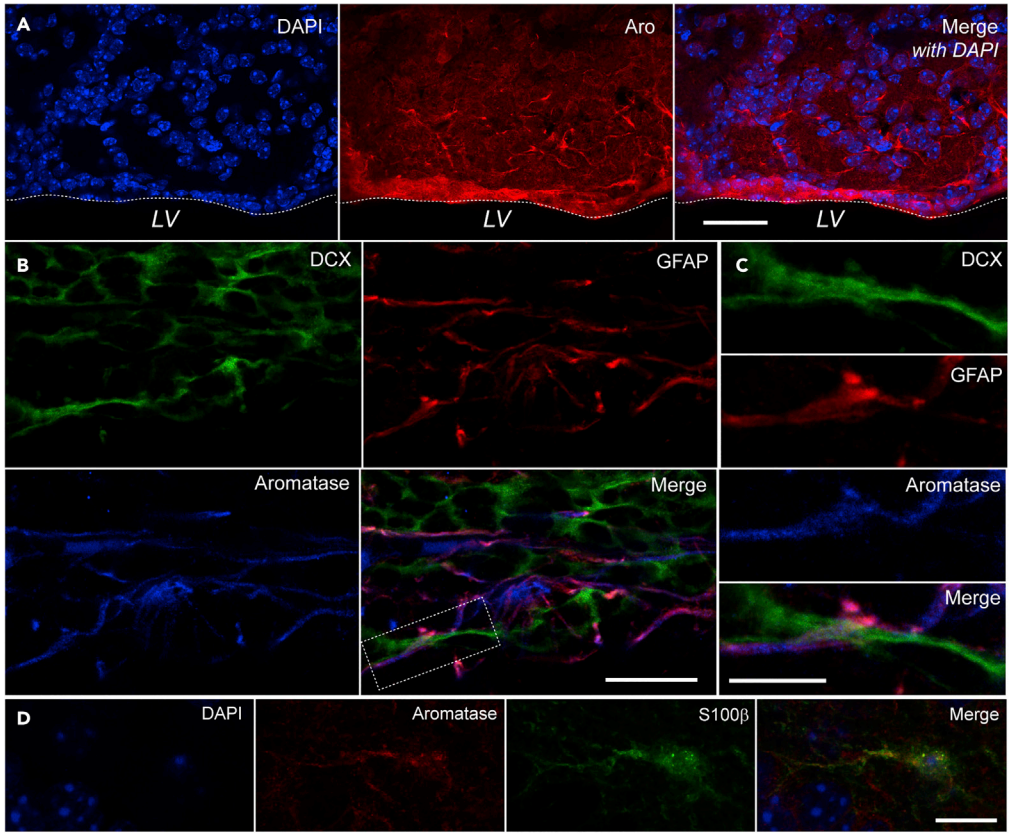

Figure 5. Aromatase Is Expressed in the Stem Cell Niche and in the RMS

(A) Fluorescence images of aromatase immunofluorescence taken from the V-SVZ of an adult female mouse demonstrating that aromatase is also expressed within the stem cell niche. The dotted line represents the border separating the ventricle from the V-SVZ area.

(B) Confocal images of triple fluorescence in the RMS of an adult female mouse brain to analyze colocalization of aromatase (rb), GFAP (ms), and DCX (gp). Merged images show that aromatase is expressed in GFAP-positive astrocytes ensheathing the migrating neuroblasts. No expression is found in DCX-positive migrating neuroblasts.

(C) Higher-magnification image of (B) showing the coexpression of aromatase and GFAP. Note that DCX-positive structures are negative for aromatase.

(D) S100β is a glial-specific marker and is expressed primarily by astrocytes. Confocal images of double fluorescence in the RMS of an adult female mouse brain show that aromatase is expressed in S100β-positive cells. LV, lateral ventricle. Scale bars: 50 μm in (A), 20 μm in (B), and 10 μm in (C and D).

thus each animal generated explants for both conditions. G15 clearly inhibited the outgrowth from the explants (see Figure 6B). Accordingly, following G15 treatment we observed a significant augmentation in the number of explants with lower grades (see Figure 6B).

As the blockade of GPER1 obviously results in inhibition of migration our results strongly point to an involvement of GPER1 in the migration of V-SVZ-derived cells. It is very likely, that astrocytes in the RMS and V-SVZ provide the specific ligand estradiol.

Ras-Induced p21 Is Involved in GPER1 Signaling in V-SVZ Matrigel Cultures

GPCRs mediate their signals via GTP-binding proteins. In this respect, the Ras signal transduction pathway is known for being important for cell growth, cell differentiation, and cell motility (Bar-sagi and Hall, 2000) and serves as a molecular shift to switch on/off cellular processes. To test whether GPER1 signaling in V-SVZ cultures is mediated via Ras (gene name nRas) we collected the tissue after migration for qPCR analysis and analyzed changes regarding the expression profiles of Ras (Figure 7A). The experiments revealed a significant reduction of nRas expression cultures treated with G15 when compared with the controls (Figure 7A). The findings indicate that under physiological conditions nRas may mediate GPER1 signaling in V-SVZ

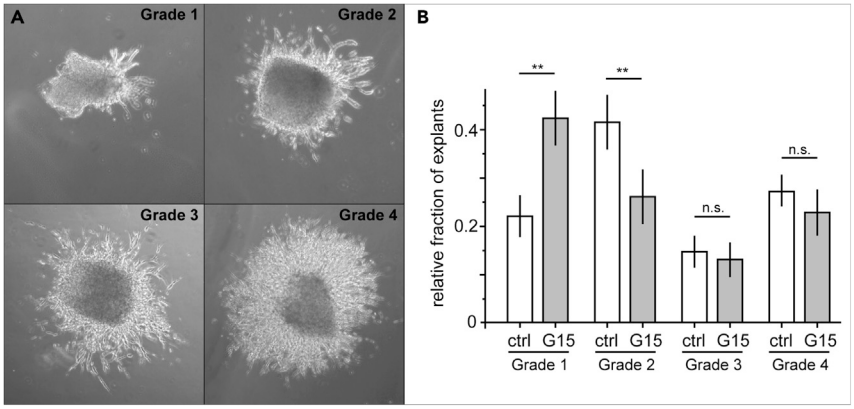

Figure 6. Blocking of GPER1 with G15 Leads to a Decrease in Migration of V-SVZ-Derived Explants

(A) Light microscopic images showing examples of explant grades.

(B) Graph showing the relative fraction of control and G15-treated explants in each grade per animal. Bars show mean ± standard error. A repeated measures two-way ANOVA on ranks was performed on the relative fractions (treatment: DF = 17, F-value = 1.070, $p = 0.315$; grade: DF = 15, F-value = 11.972, $p < 0.001$; interaction: DF = 15, F-value = 4.210, $p = 0.024$). Please note a significant difference (Scheffe post hoc test) when comparing the fraction of control with G15-treated explants in grade 1 (DF = 51, test-value = 2.91, $p = 0.005$) and grade 2 (DF = 51, test-value = 2.147, $p = 0.036$). No significant difference was found within grade 3 (DF = 51, test-value = 0.179, $p = 0.858$) and grade 4 (DF = 51, test-value = 0.5834, $p = 0.562$). Level of significance $p > 0.05$ (n.s.), $^{**}p < 0.01$.

cultures, It has been shown that activation of Ras can lead to an increase of cytosolic p21, a cyclin-dependent kinase inhibitor (Lee and Helfman, 2004; Romanov et al., 2012). GPER1 activation, in turn, is linked to an upregulation of p21 (Chan et al., 2010). Besides its known function as a negative regulator of cell cycle, recent findings have demonstrated that p21 is also involved in the regulation of cell proliferation (Bertoli et al., 2013; Zaldua et al., 2016), differentiation (de Renty et al., 2014), and control of the actin cytoskeleton and cell migration (Besson et al., 2004). Given this background, we hypothesized whether p21 levels are also affected when inhibiting GPER1 signaling with G15 in our V-SVZ culture system. We, therefore, performed qPCR studies to analyze p21 levels of explant cultures treated with G15. Similar to the observed G15 effect on Ras expression we found a significant decrease in p21 expression after blocking GPER1 with G15 (Figure 7B). These results indicate that GPER1 signaling in V-SVZ explant cultures affects nRas and p21 expression levels, which may account for the effects observed in cultures treated with G15.

The Ratio of p-Cofilin/Cofilin Is Increased in Samples Treated with G15

Once differentiating precursors of the V-SVZ are in the type A cell status, these neuroblasts start to migrate out of their germinal niche. Cell division, differentiation, and, in particular, migration are processes that are linked to changes of the cytoskeleton. Actin depolymerizing factor/cofilin family members are able to bind G-actin monomers and depolymerize actin filaments, a prerequisite for migration and chemotaxis of cells (Meberg and Bamburg, 2000; Gungabissoon and Bamburg, 2003; Ghosh et al., 2004). Recently, it was shown that p21 is involved in Ras-induced inhibition of the ROCK/LIMK/cofilin pathway (Lee and Helfman, 2004). As we observed Ras and p21 to be downregulated in response to G15 treatment in V-SVZ explants, these findings prompted us to analyze whether GPER1 inhibition also alters cofilin dynamics. As cofilin destabilizes the cytoskeleton, whereas the phosphorylated form of cofilin (p-cofilin) stabilizes it (Meberg and Bamburg, 2000; Gungabissoon and Bamburg, 2003), we examined explants by western blot analysis to determine the ratio of cofilin and p-cofilin in cultures treated with G15-treated and non-treated cultures. Consistent with our findings on Ras and p21 expression, we observed that G15-treated V-SVZ cultures showed a significant shift in the ratio of p-cofilin/cofilin toward higher p-cofilin levels. Thus, the dynamics of the cytoskeleton are impaired in cultures with a blocked GPER1 (Figure 8A [representative bands from cofilin/p-cofilin western blots] and Figure 8B; see Figure S3 for full immunoblots with all markers of molecular weight, showing that every antibody labels only one single band). To exclude the possibility that potential residues of Matrigel could alter our results we performed control western blots with Matrigel probes (Figure 8C).

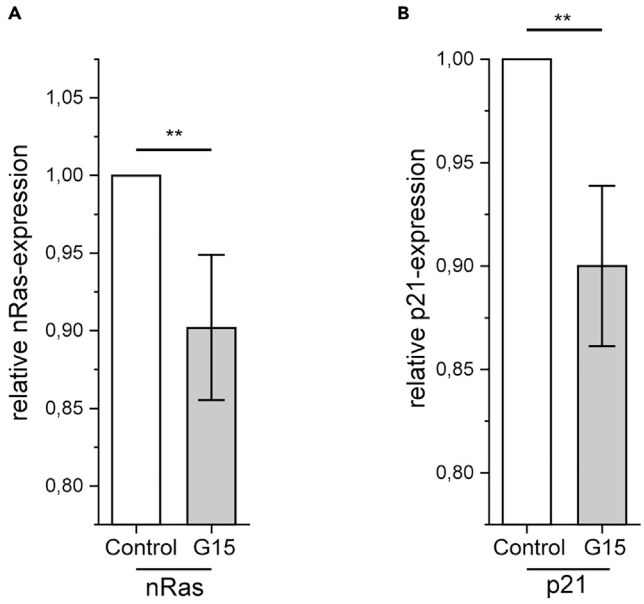

Figure 7. Blocking of GPER1 with G15 Leads to a Decrease in Expression of nRas and p21

(A and B) Graph demonstrating the expression of nRas (A) and p21 (B) in control (white bars) and G15 (gray bars)-treated cultures. qPCR data show that incubation of V-SVZ-derived cultures with the GPER1 antagonist G15 leads to a significant reduction of nRas expression when compared with control cultures (Mann-Whitney U test: $U = 16$, $n1 = n2 = 7$, $p = 0.021$). Similar to the observed G15 effect on Ras expression we found a significant decrease in p21 expression after blocking GPER1 with G15 tissue (Mann-Whitney U test: $U = 25$, $n1 = n2 = 5$, $p = 0.008$). Every experiment was performed at least three times. PCR efficiency was 1.8472 for Hprt, 1.7431 for nRas, and 1.7263 for p21. Statistical evaluation was performed using the non-parametric Wilcoxon-Mann-Whitney test. Level of significance $^{**}p < 0.01$.

To further substantiate our results we controlled our p-cofilin versus cofilin readout by analyzing Tesk1 and chronophin levels in our culture system. Both proteins are well-known regulators of cofilin with Tesk1 inactivating cofilin by phosphorylation (Toshima et al., 2001) and chronophin activating it by de-phosphorylation (Gohla et al., 2005). In accordance with our finding that G15 treatment results in an increase in the ratio of p-cofilin/cofilin we observed that G15 leads to an increase in Tesk1 expression (Figures 8D and 8E), whereas chronophin expression is not changed or only slightly reduced (Figures 8G and 8H; see Figure S3 for full immunoblots with all markers of molecular weight). No signal was seen in pure Matrigel controls (Figures 8F and 8I). As a result, our results show that blocking of GPER1 in V-SVZ cultures by G15 results in a decrease of Ras and p21 expression levels and accordingly an increase in the ratio of p-cofilin/cofilin, thereby stabilizing the cytoskeleton.

DISCUSSION

GPER1 Is Strongly Expressed by Cells in the V-SVZ

The mechanisms controlling neurogenesis, differentiation, and migration processes in the V-SVZ are not yet fully understood. Although it is generally accepted that steroids such as estrogens influence cell proliferation in the germinal region of the hippocampal dentate gyrus, their role as a modulator in the stem cell niche of the V-SVZ is so far controversial. It has been shown that estradiol can stimulate progenitor cell division in the V-SVZ of the embryonic neocortex (Martínez-Cerdeño et al., 2006). Other studies, however, deny an involvement of estrogens in cell proliferation and point to prolactin as a player in the regulation of V-SVZ-derived progenitor fate (Shingo et al., 2003).

In this study, we demonstrate a novel role of GPER1 in the regulation of V-SVZ-derived neuroblast migration. For our experiments we used female animals only, as estrogenic actions in the brain have been shown to be sex specific (for review see Brandt and Rune, 2019). It was shown that in the hippocampus locally synthesized estradiol regulates dendritic spine and spine synapse density and long-term potentiation only in females but not in males (Vierk et al., 2012), whereas locally synthesized dihydrotestosterone regulates these parameters of synaptic plasticity in males but not in females (Brandt et al., 2019). Performing

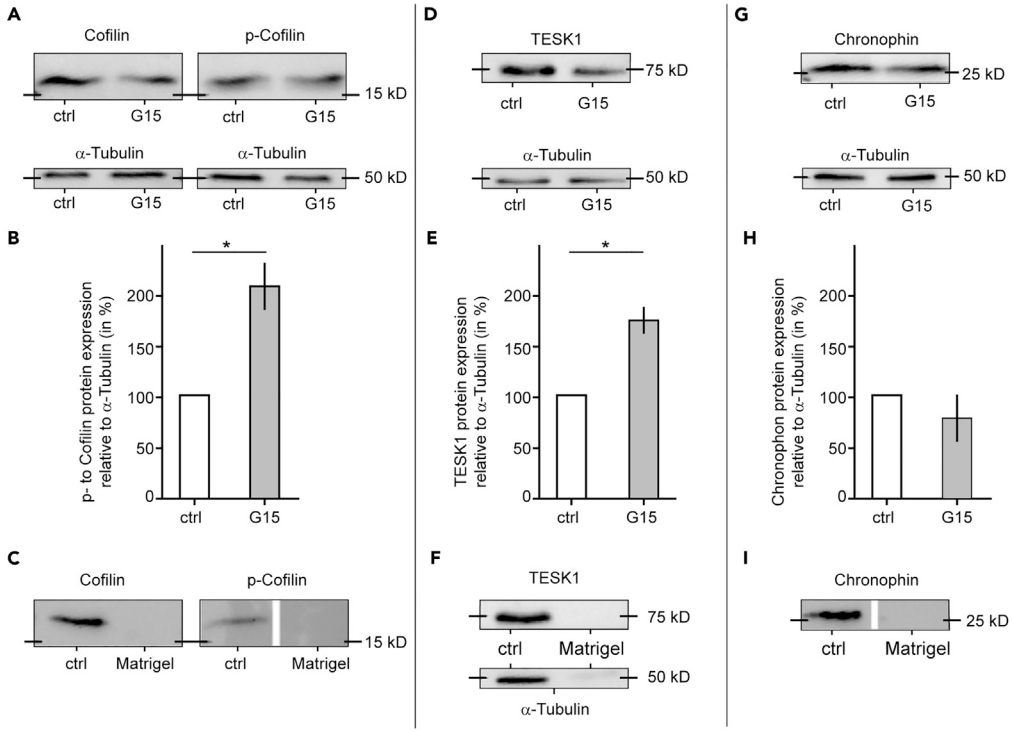

Figure 8. Treatment of Explants with G15 Leads to an Increase in the Ratio of p-Cofilin/n-Cofilin and Influences the Expression of Regulators of Cofilin

(A) Western blots showing the expression of cofilin and p-cofilin from control and samples treated with G15.

(B and C) (B) Graph showing that incubation with G15 (gray bar) leads to an increase in ratio of p-cofilin/cofilin relative to α-tubulin (Mann-Whitney U test: U = 1, n1 = n2 = 5, p = 0.022). (C) Western blots showing as a control of the antibodies used that no bands were visible in pure Matrigel preparations.

(D) Western blot showing expression of TESK1, a regulator of cofilin, which inactivates the molecule by phosphorylation, in control and G15-treated samples.

(E) Graph showing that treatment from explants with G15 leads to a significant increase in TESK1 expression (Mann-Whitney U test: U = 0, n1 = n2 = 4, p = 0.030).

(F) Western blots showing as a control of the TESK1 antibody used that no bands were visible in pure Matrigel preparation.

(G) Western blot showing expression of chronophin in control and G15-treated samples.

(H and I) (H) In contrast to the TESK1 expression, the expression of chronophin, a regulator of cofilin, which activates the molecule by de-phosphorylation, is not significantly altered (Mann-Whitney U test: U = 9 n1 = n2 = 5, p = 0.531). (I) Western blot showing as a control of the Chronophin antibody used that no bands were visible in pure Matrigel preparation.

immunohistochemistry with markers labeling the different cell types within the V-SVZ we found GPER1 expression in all cell types of the stem cell niche in principal. However, not every cell expressing one of the marker molecules was also positive of GPER1, suggesting that only a subset of each cell type expresses the receptor. Recently, it was shown that type B astrocytes as well as type C cells and neuroblasts gain and lose their marker expression profile throughout their lineage progression (Mamber et al., 2013), showing that the expression pattern may overlap at the transition from one cell type to another. It is tempting, therefore, to speculate that GPER1 expression might be transient as well, depending on the developmental state of the cells. Along these lines, GPER1 often shows a polarized expression in the V-SVZ, in contrast to even staining of the cell membrane in non-dividing and differentiated cells. Polarized expression of receptors during migration has been proposed to enable cells to respond to gradients of chemical attractants (Nieto et al., 1997; Witze et al., 2008). For chemokine receptors it was demonstrated that a polarized redistribution of receptors initiates lymphocyte migration (Nieto et al., 1997).

Within the V-SVZ it is the type A neuroblast that starts migrating toward the OB. Our data suggest, however, that cells do not rely on GPER1 for reaching the OB, their final destination, as migratory type A cells

do not express this receptor in the RMS. The exit from the cell cycle, which includes proliferation and differentiation, takes place in the neurogenic niche before migration is initiated. The question of how these signals are coordinated during cell fate determination has been extensively studied in progenitor cells in *Drosophila* and *C. elegans*, where cell fate is influenced by asymmetric cell divisions. This also holds true for mammalian cells (for review see Pham et al., 2014), in particular during development of the brain. During brain development the progenitor pool is increased by symmetric cell divisions, whereas subsequent asymmetric divisions in neurogenic niches coordinate self-renewal with differentiation of cells committed to the neuronal lineage (Zhong et al., 1996). It was proposed that polarized expression of cellular components underlie asymmetric cell division and thus cell fate and cell positioning (Betschinger and Knoblich, 2004; Suzuki and Ohno, 2006; Goldstein, and Macara, 2007; Knoblich, 2008). Regarding the polarized expression of GPER1 in different precursors of the germinal region it could well be that GPER1 expression contributes to these processes.

Astrocytes Are Able to Supply GPER1-Positive Cells in the Germinal Niche and ERα-Positive Cells in the RMS with Estradiol

Since the discovery of aromatase expression in the central nervous system (Naftolin et al., 1971) its activity was first detected in brain areas that are involved in reproductive functions and behaviors, e.g., the hypothalamus (Flores et al., 1973; Roselli et al., 1985). However, in the last decade aromatase has been identified in many other brain regions such as the hippocampus, visual cortex, and temporal cortex (Rune and Frotscher, 2005; Yague et al., 2006; Azcoitia et al., 2011; Saldanha et al., 2011). Using immunohistochemistry for aromatase we provide evidence that the last enzyme in estradiol synthesis is expressed by astrocytes, which sheath the cells of the V-SVZ and the migrating precursors in the RMS. Thus locally synthesized estradiol may serve as a ligand for cells expressing E2 receptors. Our data showing expression of aromatase in glial cells are in contrast to previous studies of aromatase expression in the rat OB (Hoyk et al., 2014), where the enzyme is expressed exclusively in neurons in the main OB. Aromatase-expressing astrocytes, however, were observed in many brain regions under physiological conditions (Kretz et al., 2004; Yague et al., 2006, 2008) and after injury, highlighting the neuroprotective capacities of the enzyme (Garcia-Segura et al., 1999).

Adult type A cells in the RMS are negative for GPER1 but express the classical genomic receptor ERα. GPER1 immunoreactivity was only seen in type A cells in the V-SVZ and at the beginning of the RMS. This pattern of immunoreactivity strongly suggests that different cells persisting and/or migrating from the V-SVZ exhibit different subsets or combinations of E2 receptors. This different receptor load may enable cells to respond differentially to E2, depending on their developmental stage with regard to migration, cell division, differentiation, and migration. Our finding of aromatase-positive astrocytes in the V-SVZ as well as in the RMS suggests an important role of E2 in the differentiation and migration of V-SVZ-derived cells in the female brain.

GPER1 Is Involved in the Modulation of Cofilin via Ras-Mediated Alteration of p21 Expression

In the last decade several studies analyzed the effect of GPER1 activation in various cell lines with discrepant results. Some studies showed that GPER1 activation leads to growth inhibition (Chan et al., 2010), whereas others postulated a growth-promoting action of GPER1 activation (Vivacqua et al., 2006a, 2006b; Albanito et al., 2007). The modulation of cell growth by GPER1 activation is transmitted by modulations of p21 expression (Chan et al., 2010). The cell cycle regulator p21 was originally thought to inhibit cell cycle progression (Abukhdeir and Park, 2008; Dulic et al., 1998). The phosphorylated form of p21, however, controls the reorganization of the actin cytoskeleton, which is also required for cell shape alterations and cell migration (Besson et al., 2004). The control of cytoskeleton organization via p21 takes place through inhibition of the ROCK/LIMK/cofilin pathway (Lee and Helfman, 2004). We found in our study a significant reduction of p21 in V-SVZ cultures treated with G15, and this reduction was paralleled by an increase in the ratio of p-cofilin/cofilin. Our data are in line with studies showing that an elevation of p21 levels results in a decrease in the phosphorylation level of cofilin and in turn to polymerization of actin (Lee and Helfman, 2004), which is a prerequisite for cell migration and cell shape alterations. Consequently, cofilin has been shown to be associated with neuronal migration disorders and cell cycle control in the cerebral cortex (Bellenchi et al., 2007). However, it needs to be considered that the V-SVZ is not a static construct. After the exit from the cell cycle, cells need to reorganize their position within the V-SVZ resulting in a permanent modulation of the germinal niche. This is especially important as cells in this region pass through different developmental states (from type B to type C to type A cells) with every cell being positioned in a special region within the germinal niche also depending on their final positioning within the OB (Mirzadeh et al., 2008; Lim and Alvarez-Buylla, 2014). It has been shown that cofilin is active at the leading edge of locomotory protrusions of migrating cells (Bravo-Cordero et al., 2013). In addition, inhibition of its activity causes

defects in protrusion, cell polarity, and chemotaxis (Delorme et al., 2007; Mouneimne et al., 2006; Sidani et al., 2007). Hence changes in the p-cofilin/cofilin ratio can influence cell cycle exit decisions as well as the positioning within the germinal niche. In other systems it was shown that E2 via GPER and ER is able to induce neuritogenesis (Denley et al., 2018), which also depends on remodeling of the cytoskeleton. Thus in the V-SVZ polarized GPER1 signaling could be a component influencing differentiation and/or positioning of cells.

In summary, the evidence presented in this study reveals a role of the ER GPER1 in the control of SVZ-derived neuroblast differentiation and migration, by influencing p21 expression and thereby modulating the ratio of p-cofilin/cofilin during development. As the V-SVZ is the biggest region with ongoing neurogenesis in the adult brain, which generates new neurons for the OB throughout life, the mechanism observed during development may also apply for the adult V-SVZ. The activation of the same signaling pathway in distinct V-SVZ-derived cells may induce different biological responses required to control the multiple steps of neurogenesis including progression along the cell line and cell migration in this germinal niche.

Limitations of the Study

All experiments in this study were carried out on female animals. It is therefore not yet possible to make a cross-gender statement on the function of the examined ER GPER1 in migration of V-SVZ-derived cells.

METHODS

All methods can be found in the accompanying Transparent Methods supplemental file.

SUPPLEMENTAL INFORMATION

Supplemental Information can be found online at https://doi.org/10.1016/j.isci.2020.101077.

ACKNOWLEDGMENTS

We thank Drs. U. Wehrenberg and D. Junghans for critically reading and improving the manuscript, C. Schröder for excellent technical assistance, and A.V. Failla from the UKE Microscopy Imaging Facility for helpful support.

AUTHOR CONTRIBUTIONS

I.H.: Conceptualization, Methodology, Investigation, Writing – Original Draft, Visualization, Formal Analysis, Supervision; M.A.S.: Conceptualization, Methodology, Visualization, Investigation; M.A., Conceptualization, Methodology, Visualization, Formal Analysis; G.M.R.: Conceptualization, Writing – Review & Editing, Supervision, Funding Acquisition.

DECLARATION OF INTERESTS

The authors declare no competing interests.

Received: July 31, 2019
Revised: December 1, 2019
Accepted: April 14, 2020
Published: May 22, 2020

REFERENCES

Abukhdeir, A.M., and Park, B.H. (2008). P21 and p27: roles in carcinogenesis and drug resistance. Expert Rev. Mol. Med. *10*, e19.

Albanito, L., Madeo, A., Lappano, R., Vivacqua, A., Rago, V., Carpino, A., Oprea, T.I., Prossnitz, E.R., Musti, A.M., Andò, S., and Maggiolini, M. (2007). G protein-coupled receptor 30 (GPR30) mediates gene expression changes and growth response to 17beta-estradiol and selective GPR30 ligand G-1 in ovarian cancer cells. Cancer Res. *67*, 1859–1866.

Apple, D.M., Solano-Fonseca, R., and Kokovay, E. (2017). Neurogenesis in the aging brain. Biochem. Pharmacol. *141*, 77–85.

Arnal, J.F., Lenfant, F., Metivier, R., Flouriot, G., Henrion, D., Adlanmerini, M., Fontaine, C., Gourdy, P., Chambon, P., Katzenellenbogen, B., and Katzenellenbogen, J. (2017). Membrane and nuclear estrogen receptor alpha actions: from tissue specificity to medical implications. Physiol. Rev. *9*, 1045–1087.

Azcoitia, I., Yague, J.G., and Garcia-Segura, L.M. (2011). Estradiol synthesis within the human brain. Neuroscience *191*, 139–147.

Banasr, M., Hery, M., Brezun, J.M., and Daszuta, A. (2001). Serotonin mediates oestrogen stimulation of cell proliferation in the adult dentate gyrus. Eur. J. Neurosci. *14*, 1417–1424.

Bar-sagi, D., and Hall, A. (2000). Ras and Rho GTPases: a family reunion. Cell *10*, 227–238.

Bellenchi, G.C., Gurniak, C.B., Perlas, E., Middei, S., Ammassari-Teule, M., and Witke, W. (2007). N-cofilin is associated with neuronal migration disorders and call cycle control in the cerebral cortex. Genes Dev. *21*, 2347–2357.

Bertoli, C., Skotheim, J.M., and de Bruin, R.A.M. (2013). Control of cell cycle transcription during G1 and S phases. Nat. Rev. Mol. Cell Biol. *14*, 518–528.

Besson, A., Assoian, R.K., and Roberts, J.M. (2004). Regulation of the cytoskeleton: an oncogenic function for CDK inhibitors? Nat. Rev. Cancer *4*, 948–955.

Bondar, G., Kuo, J., Hamid, N., and Micevych, P. (2009). Estradiol-induced estrogen receptor-alpha trafficking. J. Neurosci. *29*, 15323–15330.

Brandt, N., Vierk, R., Fester, L., Anstötz, M., Zhou, L., Heilmann, L.F., Kind, S., Steffen, P., and Rune, G.M. (2019). Sex-specific difference of hippocampal synaptic plasticity in response to sex neurosteroids. Cereb. Cortex *30*, 2627–2641.

Brännvall, K., Korhonen, L., and Lindholm, D. (2002). Estrogen-receptor-dependent regulation of neural stem cell proliferation and differentiation. Mol. Cell. Neurosci: *21*, 512–520.

Brandt, N., and Rune, G.M. (2019). Sex-dependency of oestrogen-induced structural synaptic plasticity: inhibition of aromatase versus application of estradiol in rodents. Eur. J. Neurosci. https://doi.org/10.1111/ejn.14541.

Bravo-Cordero, J.J., Sharma, V.P., Roh-Johnson, M., Chen, M., Eddy, R., Condeelis, J., and Hodgson, L. (2013). Spatial regulation of RhoC activity defines protrusion formation in migrating cells. J. Cell. Sci. *126*, 3356–3369.

Betschinger, J., and Knoblich, J.A. (2004). Dare to be dierent: asymmetric cell division in Drosophila, C. elegans and vertebrates. Curr. Biol. *14*, R674–R685.

Brock, O., Keller, M., Veyrac, A., Douhard, Q., and Bakker, J. (2010). Short term treatment with estradiol decreases the rate of newly generated cells in the subventricular zone and main olfactory bulb of adult female mice. Neuroscience *166*, 368–376.

Chan, Q.K., Lam, H.M., Ng, C.F., Lee, A.Y., Chan, E.S., Ng, H.K., Ho, S.M., and Lau, K.M. (2010). Activation of GPR30 inhibits the growth of prostate cancer cells through sustained activation of Erk1/2, c-jun/c-fos-dependent upregulation of p21, and induction of G (2) cell-cycle arrest. Cell Death Differ. *17*, 1511–1523.

Cheng, S.B., Quinn, J.A., Graeber, C.T., and Filardo, E.J. (2011). Down-modulation of the G-protein-coupled estrogen receptor, GPER, from the cell surface occurs via a trans-Golgi-proteasome pathway. J. Biol. Chem. *286*, 22441–22455.

Davis, P., McEwen, B.S., and Pfaff, D.W. (1979). Localized behavioral effects of tritiated estradiol implants in the ventromedial hypothalamus of female rats. Endocrinology *104*, 898–903.

Delorme, V., Machacek, M., DerMardirossian, C., Anderson, K.L., Wittmann, T., Hanein, D., Waterman-Storer, C., Danuser, G., and Bokoch, G.M. (2007). Cofilin activity downstream of Pak1 regulates cell protrusion efficiency by organizing lamellipodium and lamella actin networks. Dev. Cell *13*, 646–662.

Denley, M.C.S., Gatford, N.J.F., Sellers, K.J., and Srivastava, D.P. (2018). Estradiol and the development of the cerebral cortex: un unexpected role. Front. Neurosci *12*, 245.

Dennis, M.K., Burai, R., Ramesh, C., Petrie, W.K., Alcon, S.N., Nayak, T.K., Bologa, C.G., Leitao, A., Brailoiu, E., Deliu, E., et al. (2009). In vivo effects of a GPR30 antagonist. Nat. Chem. Biol. *5*, 421–427.

de Renty, C., DePamphillis, M.L., and Ullah, Z. (2014). Cytoplasmic Localization of p21 protects trophoblast giant cells from DNA damage induced apoptosis. PLoS One *9*, e97434.

Dixon, K.J., Turbic, A., Turnley, A.M., and Liebl, D.J. (2017). Explant methodology for analyzing neuroblast migration. Bio Protocol *7*, e2249.

Doetsch, F., García-Verdugo, J.M., and Alvarez-Buylla, A. (1997). Cellular composition and three-dimensional organization of the subventricular germinal zone in the adult mammalian brain. J. Neurosci. *17*, 5046–5061.

Du, G.Q., Zhou, L., Chen, X.Y., Wan, X.P., and He, Y.Y. (2012). The G protein-coupled receptor GPR30 mediates the proliferative and invasive effects induced by hydroxytamoxifen in endometrial cancer cells. Biochem. Biophys. Res. Commun. *420*, 343–349.

Dulic, V., Stein, G.H., Far, D.F., and Ree, S.I. (1998). Nuclear accumulation of p21Cip1 at the onset of mitosis: a role at the G2/M-phase transition. Mol. Cell Biol. *18*, 546–557.

Fester, L., Ribeiro-Gouveia, V., Prange-Kiel, J., von Schassen, C., Böttner, M., Jarry, H., and Rune, G.M. (2006). Proliferation and apoptosis of hippocampal granule cells require local oestrogen synthesis. J. Neurochem. *97*, 1136–1144.

Filardo, E.J., Quinn, J.A., Frackelton, A.R., Jr., and Bland, K.I. (2002). Estrogen action via the G protein-coupled receptor, GPR30: stimulation of adenylyl cyclase and cAMP-mediated attenuation of the epidermal growth factor receptor-to-MAPK signaling axis. Mol. Endocrinol. *16*, 70–84.

Filardo, E.J., and Thomas, P. (2012). Minireview: G protein-coupled estrogen receptor-1, GPER-1: its mechanism of action and role in female reproductive cancer, renal and vascular physiology. Endocrinology *153*, 2953–2962.

Flores, F., Naftolin, F., Ryan, K.J., and White, R.J. (1973). Estrogen formation by the isolated perfused rhesus monkey brain. Science *180*, 1074–1075.

Fuentealba, L.C., Obernier, K., and Alvarez-Buylla, A. (2012). Adult neural stem cells bridge their niche. Cell Stem Cell *10*, 698–708.

Funakoshi, T., Yanai, A., Shinoda, K., Kawano, M.M., and Mizukami, Y. (2006). G protein-coupled receptor 30 is an estrogen receptor in the plasma membrane. Biochem. Biophys. Res. Comm. *346*, 904–910.

Garcia-Segura, L.M., Wozniak, A., Azcoitia, I., Rodriguez, J.R., Hutchison, R.E., and Hutchison, J.B. (1999). Aromatase expression by astrocytes after brain injury: implications for local estrogen formation in brain repair. Neuroscience *89*, 567–578.

Ghosh, M., Song, X., Mouneimne, G., Sidani, M., Lawrence, D.S., and Condeelis, J.S. (2004). Cofilin promotes actin polymerization and defines the direction of cell motility. Science *304*, 743–746.

Gohla, A., Birkenfeld, J., and Bokoch, G.M. (2005). Chronophin, a novel HAD-type serine protein phosphatase, regulates cofilin-dependent actin dynamics. Nat. Cell Biol. *7*, 21–29.

Goldstein, B., and Macara, I.G. (2007). The PAR proteins: fundamental players in animal cell polarization. Dev. Cell. *13*, 609–622.

Gungabissoon, R.A., and Bamburg, J.R. (2003). Regulation of growth cone actin dynamics by ADF/cofilin. J. Histochem. Cytochem. *51*, 411–420.

Hoyk, Z., Varga, C., and Parducz, A. (2006). Estrogen-induced region specific decrease in the density of 5-bromo-2-deoxyuridine-labeled cells in the olfactory bulb of adult female rats. Neuroscience *141*, 1919–1924.

Hoyk, Z., Csákvári, E., Gyenes, A., Siklós, L., Harada, N., and Párducz, A. (2014). Aromatase and estrogen receptor beta expression in the rat olfactory bulb: neuroestrogen action in the first relay station of the olfactory pathway? Acta Neurobiol. Exp. *74*, 1–14.

Horvath, T.L., and Wikler, K.C. (1999). Aromatase in developing sensory systems of the rat brain. J. Neuroendocrinol. *11*, 77–84.

Isgor, C., and Watson, S.J. (2005). Estrogen receptor alpha and beta mRNA expressions by proliferating and differentiating cells in the adult rat dentate gyrus and subventricular zone. Neuroscience *134*, 847–856.

Jensen, E.V., and DeSombre, E.R. (1973). Estrogen-receptor interaction. Science *182*, 126–134.

Kanageswaran, N., Nagel, M., Scholz, P., Mohrhardt, J., Gisselmann, G., and Hatt, H. (2016). Modulatory effects of sex steroids progesterone and estradiol on odorant evoked responses in olfactory receptor neurons. PLoS One *11*, e0159640.

Knoblich, J.A. (2008). Mechanisms of asymmetric stem cell division. Cell *132*, 583–597.

Kretz, O., Fester, L., Wehrenberg, U., Zhou, L., Brauckmann, S., Zhao, S., Prange-Kiel, J., Naumann, T., Jarry, H., Frotscher, M., and Rune, G.M. (2004). Hippocampal synapses depend on hippocampal estrogen synthesis. J. Neurosci. *24*, 5913–5921.

Larsen, C.M., Kokay, I.C., and Grattan, D.R. (2008). Male pheromones initiate prolactin-induced neurogenesis and advance maternal behavior in female mice. Horm. Behav. *53*, 509–517.

Larsen, C.M., and Grattan, D.R. (2010). Prolactin-induced mitogenesis in the subventricular zone of the maternal brain during early pregnancy is essential for normal postpartum behavioral responses in the mother. Endocrinology *151*, 3805–3814.

Lee, S., and Helfman, D.M. (2004). Cytoplasmic p21^{Cip1} is involved in ras-induced inhibition of the ROCK/LIMK/Cofilin Pathway. J. Biol. Chem. *279*, 1885–1891.

Lennington, J.B., Yang, Z., and Conover, J.C. (2003). Neural stem cells and the regulation of adult neurogenesis. Reprod. Biol. Endocrinol. *1*, 99.

Li, Y., Jia, Y., Bian, Y., Tong, H., Qu, J., Wang, K., and Wan, X.P. (2019). Autocrine motility factor promotes endometrial cancer progression by targeting GPER-1. Cell Commun. Signal. *17*, 22.

Lim, D.A., and Alvarez-Buylla, A. (2014). Adult neural stem cells stake their ground. Trends Neurosci. *37*, 563–571.

Lisk, R.D., and Suydam, A.J. (1967). Sexual behavior patterns in the prepubertally castrate rat. Anat. Rec. *157*, 181–189.

Lois, C., and Alvarez-Buylla, A. (1994). Long-distance neuronal migration in the adult mammalian brain. Science *264*, 1145–1148.

Luskin, M.B. (1993). Restricted proliferation and migration of postnatally generated neurons derived from the forebrain subventricular zone. Neuron *11*, 173–189.

Mak, G.K., Enwere, E.K., Gregg, C., Pakarainen, T., Poutanen, M., Huhtaniemi, I., and Weiss, S. (2007). Male pheromone-stimulated neurogenesis in the adult female brain: possible role in mating behavior. Nat. Neurosci. *10*, 1003–1011.

Mak, G.K., and Weiss, S. (2010). Paternal recognition of adult offspring mediated by newly generated CNS neurons. Nat. Neurosci. *13*, 753–758.

Mamber, C., Kozareva, D.A., Kamphuis, W., and Hol, E.M. (2013). Shades of gray: the delineation of marker expression within the adult rodent subventricular zone. Prog. Neurobiol. *111*, 1–16.

Marino, M., Ascenzi, P., and Acconcia, F. (2006). S-palmitoylation modulates estrogen receptor alpha localization and functions. Steroids *71*, 298–303.

Marrocco, J., and McEwen, B.S. (2016). Sex in the brain: hormones and sex differences. Dialogues Clin. Neurosci. *18*, 373–383.

Martínez-Cerdeño, V., Noctor, S.C., and Kriegstein, A.R. (2006). Estradiol stimulates progenitor cell division in the ventricular and subventricular zones of the embryonic neocortex. Eur. J. Neurosci. *24*, 3475–3488.

McEwen, B.S., and Milner, T.A. (2017). Understanding the broad influence of sex hormones and sex differences in the brain. J. Neurosci. Res. *95*, 24–39.

Meberg, P.J., and Bamburg, J.R. (2000). Increase in neurite outgrowth mediated by overexpression of actin depolymerizing factor. J. Neurosci. *20*, 2459–2469.

Mirzadeh, Z., Merkle, F.T., Soriano-Navarro, M., Garcia-Verdugo, J.M., and Alvarez-Buylla, A. (2008). Neural stem cells confer unique pinwheel architecture to the ventricular surface in neurogenic regions of the adult brain. Cell Stem Cell *3*, 265–278.

Mouneimne, G., DesMarais, V., Sidani, M., Scemes, E., Wang, W., Song, X., Eddy, R., and Condeelis, J. (2006). Spatial and temporal control of cofilin activity is required for directional sensing during chemotaxis. Curr. Biol. *16*, 2193–2205.

Mouret, A., Lepousez, G., Gras, J., Gabellec, M.M., and Lledo, P.M. (2009). Turnover of new-born olfactory bulb neurons optimizes olfaction. J. Neurosci. *9*, 12302–12314.

Naftolin, F., Ryan, K.J., and Petro, Z. (1971). Aromatization of androstenedione by limbic tissue from human fetuses. J. Endocrinol. *51*, 795–796.

Nieto, M., Frade, M.R., Sancho, D., Mellado, M., Martinez, A.C., and Sánchez-Madrid, F. (1997). Polarization of chemokine receptors to the leading edge during lymphocyte chemotaxis. J. Exp. Med. *186*, 153–158.

Pappas, T.C., Gametchu, B., and Watson, C.S. (1995). Membrane estrogen receptors identified by multiple antibody labeling and impeded-ligand binding. FASEB J. *9*, 404–410.

Pfaff, D.W. (1980). Estrogens and Brain Function (Springer-Verlag).

Pedram, A., Razandi, M., Lewis, M., Hammes, S., and Levin, E.R. (2014). Membrane-localized estrogen receptor α is required for normal organ development and function. Dev. Cell *29*, 482–490.

Pham, K., Sacirbegovic, F., and Russell, S.M. (2014). Polarized cells, polarized views: asymmetric cell division in hematopoietic cells. Front. Immunol. *5*, 26.

Ponti, G., Obernier, K., Guinto, C., Jose, L., Bonfanti, L., and Alvarez-Buylla, A. (2013a). Cell cycle and lineage progression of neural progenitors in the ventricular-subventricular zones of adult mice. Proc. Natl. Acad. Sci. U S A *110*, E1045–E1054.

Ponti, G., Obernier, K., and Alvarez-Buylla, A. (2013b). Lineage progression from stem cells to new neurons in the adult brain ventricular-subventricular zone. Cell Cycle *12*, 1649–1650.

Prange-Kiel, J., and Rune, G.M. (2006). Direct and indirect effects of estrogen on rat hippocampus. Neuroscience *138*, 765–772.

Prange-Kiel, J., Fester, L., Zhou, L., Lauke, H., Carretero, J., and Rune, G.M. (2006). Inhibition of hippocampal estrogen synthesis causes region-specific downregulation of synaptic protein expression in hippocampal neurons. Hippocampus *16*, 464–471.

Prossnitz, E.R., Oprea, T.I., Sklar, L.A., and Arterburn, J.B. (2008). The ins and outs of GPER30 a transmembrane estrogen receptor. J. Steroid Biochem. Mol. Biol. *109*, 350–353.

Razandi, M., Pedram, A., Greene, G.L., and Levin, E.R. (1999). Cell membrane and nuclear estrogen receptors (ERs) originate from a single transcript: studies of ERalpha and ERbeta expressed in Chinese hamster ovary cells. Mol. Endocrinol. *13*, 307–319.

Revankar, C.M., Cimino, D.F., Sklar, L.A., Arterburn, J.B., and Prossnitz, E.R. (2005). A transmembrane intracellular estrogen receptor mediates rapid cell signaling. Science *307*, 1625–1630.

Romanov, V.S., Pospelov, V.A., and Pospelova, T.V. (2012). Cyclin-dependent kinase inhibitor p21^{Waf1}: contemporary view on its role in senescence and oncogenesis. Biochem *72*, 575–584.

Roselli, C.E., Horton, L.E., and Resko, J.A. (1985). Distribution and regulation of aromatase activity in the rat hippothalamus and limbic system. Endocrinology *117*, 2471–2477.

Rune, G.M., and Frotscher, M. (2005). Neurosteroid synthesis in the hippocampus: role in synaptic plasticity. Neuroscience *136*, 833–842.

Saldanha, C.J., Remage-Healey, L., and Schlinger, B.A. (2011). Synaptocrine signaling: steroid synthesis and action at the synapse. Endocr. Rev. *32*, 532–549.

Samartzis, E.P., Noske, A., Meisel, A., Varga, Z., Fink, D., and Imesch, P. (2014). The G protein-coupled estrogen receptor (GPER) is expressed in two different subcellular localizations reflecting distinct tumor properties in breast cancer. PLoS One *9*, e83296.

Shingo, T., Gregg, C., Enwere, E., Fujikawa, H., Hassam, R., Geary, C., Cross, J.C., and Weiss, S. (2003). Pregnancy-stimulated neurogenesis in the adult female forebrain mediated by prolactin. Science *299*, 117–120.

Sidani, M., Wessels, D., Mouneimne, G., Ghosh, M., Goswami, S., Sarmiento, C., Wang, W., Kuhl, S., El-Sibai, M., Backer, J.M., et al. (2007). Cofilin determines the migration behavior and turning frequency of metastatic cancer cells. J. Cell Biol. *179*, 777–791.

Suzuki, A., and Ohno, S. (2006). The PAR-aPKC system: Lessons in polarity. J. Cell Sci. *119*, 979–987.

Tanapat, P., Hastings, N.B., Reeves, A.J., and Gould, E. (1999). Estrogen stimulates a transient increase in the number of new neurons in the dentate gyrus of the adult female rat. J. Neurosci. *19*, 5792–5801.

Thomas, P., Pang, Y., Filardo, E.J., and Dong, J. (2005). Identity of an estrogen membrane receptor coupled to a G protein in human breast cancer cells. Endocrinology *146*, 624–632.

Toshima, J., Toshima, J.Y., Amano, T., Yang, N., Narumiya, S., and Mizuno, K. (2001). Cofilin phosphorylation by protein kinase testicular protein kinase 1 and its role in integrin-mediated actin reorganization and focal adhesion formation. Mol. Biol. Cell *12*, 1131–1145.

Veyrac, A., and Bakker, J. (2011). Postnatal and adult exposure to estradiol differentially influences adult neurogenesis in the main and accessory olfactory bulb of female mice. FASEB *25*, 1048–1057.

Vierk, R., Glassmeier, G., Zhou, L., Brandt, N., Fester, L., Dudzinski, D., Wilkars, W., Bender, R.A., Lewerenz, M., Gloger, S., et al. (2012). Aromatase inhibition abolishes LTP generation in female but not in male mice. J. Neurosci. *32*, 8116–8126.

Vivacqua, A., Bonofiglio, D., Albanito, L., Madeo, A., Rago, V., Carpino, A., Musti, A.M., Picard, D., Andò, S., and Maggiolini, M. (2006a). 17beta-estradiol, genistein, and 4-hydroxytamoxifen induce the proliferation of thyroid cancer cells through the g protein-coupled receptor GPR30. Mol. Pharmacol. *70*, 1414–1423.

Vivacqua, A., Bonofiglio, D., Recchia, A.G., Musti, A.M., Picard, D., Andò, S., and Maggiolini, M. (2006b). The G protein-coupled receptor GPR30 mediates the proliferative effects induced by 17beta-estradiol and hydroxytamoxifen in endometrial cancer cells. Mol. Endocrinol. *20*, 631–646.

von Schassen, C., Fester, L., Prange-Kiel, J., Lohse, C., Huber, C., Bottner, M., and Rune, G.M. (2006). Oestrogen synthesis in the hippocampus: role in axon outgrowth. J. Neuroendocrinol. *18*, 847–856.

Wang, L., Andersson, S., Warner, M., and Gustafsson, J.A. (2003). Estrogen receptor (ER) beta knockout mice reveal a role for ERbeta in migration of cortical neurons in the developing brain. Proc. Natl. Acad. Sci. U S A *100*, 703–708.

Wang, W., Le, A.A., Hou, B., Lauterborn, J.C., Cox, C.D., Levin, E.R., Lynch, G., and Gall, C.M. (2018). Memory-related synaptic plasticity is sexually dimorphic in rodent hippocampus. J. Neurosci. *38*, 7935–7951.

Williams, S., Leventhal, C., Lemmon, V., Nedergaard, M., and Goldman, S.A. (1999). Estrogen promotes the initial migration and inception of NgCAM-dependent calcium-signaling by new neurons of the adult songbird brain. Mol. Cell Neurosci. *13*, 41–55.

Witze, E.S., Litman, E.S., Argast, G.M., Moon, R.T., and Ahn, N.G. (2008). Wnt5a control of cell polarity and directional movement by polarized redistribution of adhesion receptors. Science *320*, 365–369.

Wu, Y., Feng, D., Lin, J., Qu, Y., He, S., Wang, Y., Gao, G., and Zhao, T. (2018). Downregulation of G-protein-coupled receptor 30 in the hippocampus attenuates the neuroprotection of estrogen in the critical period hypothesis. Mol. Med. Rep. *17*, 5716–5725.

Yague, J.G., Muñoz, A., de Monasterio-Schrader, P., DeFelipe, J., Garcia-Segura, L.M., and Azcoitia, I. (2006). Aromatase expression in the human temporal cortex. Neuroscience *138*, 389–401.

Yague, J.G., Wang, A.C.J., Janssen, W.G.M., Hof, P.R., Garcia-Segura, L.M., Azcoitia, I., and Morrison, J.H. (2008). Aromatase distribution in the monkey temporal neocortex and hippocampus. Brain Res. *1209*, 115–127.

Young, W. (1961). The hormones and mating behavior. In Sex and Internal Secretions, W. Young, ed. (Williams and Wilkins), pp. 1173–1239.

Young, W.C., Goy, R.W., and Phoenix, C.H. (1964). Hormones and sexual behavior. Science *143*, 212–218.

Zaldua, N., Llavero, F., Artaso, A., and Gálvez, P. (2016). Rac1/p21-activated kinase pathway controls retinoblastoma protein phosphorylation and E2F transcription factor activation in B lymphocytes. FEBS J. *283*, 647–661.

Zhong, W., Feder, J.N., Jiang, M.M., Jan, L.Y., and Jan, Y.N. (1996). Asymmetric localization of a mammalian Numb homolog during mouse cortical neurogenesis. Neuron *17*, 43–53.

iScience, Volume *23*

Supplemental Information

GPER1 Signaling Initiates Migration of Female V-SVZ-Derived Cells

Iris Haumann, Muriel Anne Sturm, Max Anstötz, and Gabriele M. Rune

Transparant Methods

Ethic statements

All experiments were carried out in accordance with the German law on the use of laboratory animals (German Animal Welfare Act; project number ORG 882 by the "Amt für Verbraucherschutz, Lebensmittelsicherheit und Veterinärwesen") and were performed at the "Universitätsklinikum Hamburg Eppendorf", Dept. of Neuroanatomy. All methods described below were accomplished in accordance with the relevant guidelines and regulations.

Animals

Wild-type (wt) mice used in this study were on a C57BL/6J background and reared in accordance with the animal care guidelines of the University of Hamburg. Adult female (12-16 weeks) as well as postnatal (P4-P6) female mice were used. The day of birth was considered postnatal day (P) 0.

Immunohistochemistry

Fluorescence immunohistochemistry was performed as previously described (Hack et al., 2002; Junghans et al., 2008).

All primary antibodies used are listed below.

For vibratome sections non-specific binding sites were blocked for 1h at RT (10% normal goat serum (NGS), 0.5% Triton X-100 in PBS or 10 fetal calf serum (FCS), 0.5% Triton X-100 in PBS. The latter was used only when the primary antibody was generated in goat. The tissue was subsequently incubated overnight at 4°C with the primary antibodies (3% NGS or 10%FCS, 0.5% Triton X-100 in PBS). After several washes in PBS, sections were incubated for 1 h with fluorochrome-coupled secondary antibodies (3% NGS or 10% FCS in 1x PBS), washed in PBS and mounted (Fluorescent mounting medium, Dako).

Immunohistochemistry on paraffin sections including antigen retrieval was performed as previously described (Junghans et al, 2008). Briefly sections were de-paraffinized (XEM) and rehydrated (ethanol 100%, 90%, 70%, 50% ethanol, water). For antigen retreaval sections were incubated in citrate buffer [4,48 g/L citric acid, 10.76 g/L $Na_2PO_4.2H_2O$, 1.5% H_2O_2, 15 min, room temperature (RT)] followed by extensive washings in water, prior incubation in 550 mM Citric acid, pH 6,6 at 100° C for 20 min. After cooling down to RT sections were washed in PBS. Sections were blocked with 5% normal goat serum (NGS)/PBS or alternatively 10% fetal calf serum (FCS)/1x PBS for 1h, washed in PBS and incubated in 0.5% NGS/PBS (or 10% FCS/PBS) with the appropriate antibodies (ON, 4°C). After washing in PBS, fluorochrome-coupled secondary antibodies in 0.5% NGS/PBS or 10% FCS were applied (1h, RT). Finally, sections were washed and mounted (Fluorescent mounting medium, Dako). Pictures were taken on a Kyence Bionevo Microscope and on a Leica Laserscanning TCS SP8 microscope.

Peptide neutralization

The blocking peptide used for the ERα antibody was SC 543P. The Aromatase antibody was blocked with the immunizing peptide 3599BP (Biovision). The peptide neutralization steps were performed according to the manufacturer's manual. Briefly the antibodies were combined with a five-fold (by weight) excess of blocking peptide in 500 µl of PBS and incubated ON at 4°C. Following blocking/competition, the antibody/peptide mixture was diluted into the same blocking buffer used for the immunohistochemical procedure and used in parallel on the same tissue sections and with the same protocol as for the ERα or Aromatase antibody.

RNA Preparation

Tissue was homogenized by trituration with an insulin-needle (4-40 Micro-Fine; BD) in RLT buffer containing ß-Mercaptoethanol (Qiagen, Germany) and QIAshredder columns for PC analysis (Qiagen), according to the instructor's manual. The RNeasy Mini Kit (Qiagen) was used for mRNA isolation, including digestion with DNase I (Qiagen). Elution of mRNA was done in RNase free water.

Real time qPCR using TaqMan probes

Maxima First Strand Synthesis Kit (Thermo Scientific) was used to generate DNA, following the instructor's manual. Real time qPCR was performed using a StepOnePlusTM Real-Time PCR system (Applied Biosystems). The following TaqMan probes (Thermo Fisher, USA) were used: nRas (Mm 03053787_m1), cdkn1a (Mm 04205640_g1) and Hypoxanthin-Guanin-Phosphoribosyltransferase (Hprt; house-keeping gene;

Mm00446968_m1). PCR efficiency was 1,8472 for Hprt, 1,7431 for nRas and 1,7263 for cdkn1a. mRNA levels were calculated using the $2(-\Delta\Delta C(T))$ method according to Livak and Schmittgen (2001). Statistical evaluation was performed with SPSS (IBM) using the non-parametric Wilcoxon-Mann-Whitney Test. Significance was assigned for all tests at $p<0.05$.

Matrigel culture

Cultures of SVZ-explants were performed as described previously (Hack et al., 2002). P4-P6 brains were dissected and the forebrains were sliced frontally into 400 µm sections in ice cold Hank′s balanced salt solution (HBSS, Invitrogen) using a vibratome (Leica). From appropriate sections the SVZ was dissected out and cut into smaller pieces (100–300 µm in diameter). After mixing the SVZ-explants with 8µl of Matrigel without Phenolred (Corning) and incubation at 37°C for 10 min the polymerized gel was covered with 500 µl nutrition medium (Neurobasal A without Phenolred, 0,5x B27 supplement, 100 U/ml penicillin, 100 µg/ml streptomycin, 0.5 mM L-glutamine, Sigma) that contained either 10^{-7} M G15 to block GPER1 signaling or DMSO as control. The percentage of DMSO in medium was 0,5%. Culturing of VZ-SVZ-explants was performed on uncoated glass cover slips (12 mm) that were placed into non-treated 4 well dishes (176740, Nuclon). The cultures were maintained in a humidified atmosphere with 5% CO2 at 37°C. After 24 h focal planes of the explants were monitored on a Zeiss Primo Vert Microscope. Explant images were reconstructed with Adobe Photoshop DS5.1. Neuroblast migration was analyzed according to Dixon et al. (2017). For statistical analysis a "Repeated Measures Two-way ANOVA" on ranks was performed on the relative fractions. Level of significance was assigned at $p>0.05$ (n.s.); $p<0.05$ (*); $p<0.01$ (**); $p<0.001$(***).

Immunoblotting

SVZ derived Matrigel cultures were removed and consecutively lysed in 70 µl ice cold RIPA lysis buffer (150mM NaCl, 1% NP40, 0.5% Na-Deoxycholate, 0,1% SDS, 25mM Tris, pH 7,5, 5mM EDTA). After adding of $1/5^{th}$ volume of 5 × Laemmli buffer (0,5 M DTT, 10% SDS, 0,4 M Tris HCl, pH 6,8, 505 glycerol and bromphenolblau), probes were heated to 95 °C for 5 min and then immediately cooled on ice. Samples were separated in Laemmli running buffer (25 mM Tris Base, 192mM glycerol and 0,1% SDS) on a 10% polyacrylamide gel by gel electrophoresis (Biorad, Germany) before transferring electrophoretically to nitrocellulose membranes in transfer buffer (48mM Tris base, 29 mM glycerol, 1,28mM SDS and 20% MeOH). Next membranes were blocked with 5% bovine serum albumin (BSA) or milkpowder in PBS and 0,3% Tween for 1h at RT and incubated with primary antibodies in blocking solution at 4 °C overnight. Secondary HRP-conjugated antibodies were incubated for one hour at RT (Detection Kit: Immobilion Western, Millipore and Pierce ECL). The immunoreaction was visualized by enhanced chemiluminescence (FUSION-SL4 advanced imaging system; Vilber Lourmat, Belgium) and signal intensity (densitometry) was quantified using ImageJ software (NIH, USA). The results are presented as x-fold relative differences to control. Statistical evaluation was performed with SPSS (IBM) using the non-parametric Wilcoxon-Mann-Whitney Test. Significance was assigned for all tests at $p<0.05$.

List of unconjungated primary antibodies

Antigen	Host	Dilution	Source
GPER1	goat	1:250	Abcam (ab18512)
GPER1	rabbit	1:250	Abcam (ab39742)
ERα	rabbit	1:100	Santa Cruz Biotechnology Inc. (sc-543)
Aromatase	rabbit	1:100	Biovision (3599-100)
SOX2	rabbit	1:200	Abcam (ab97959)
Doublecortin	goat	1:1000	Santa Cruz Biotechnology Inc. (sc-8066)
Doublecortin	Gunea pig	1:1000	Merck (AB2253)
Vimentin	rabbit	1:100	Cell Signaling (#5741)

EGFR	rabbit	1:200	Abcam (ab40815)
GFAP	mouse	1:200	Sigma (G3892)
GFAP	rabbit	1:200	Dako (Z0334)
Cofilin	rabbit	1:1000	Cell Signaling (#5175)
Phospho-Cofilin (Ser3)	rabbit	1:300	Cell Signaling (#3313)
TESK1	rabbit	1:1000	Cell Signaling (#4655)
Chronophin	rabbit	1:1000	Cell Signaling (#4686)
S100ß	mouse	1:500	Sigma (S2532)

List of reagents and reference source

Reagent	**Reference source**
B27	Gibco (17504-044)
DMSO	SIGMA (D5879)
FBS (heat inactivated)	Gibco (10500-064)
G15	Tocris (3678)
10 x HBSS	Gibco (14180-146)
HEPES	Sigma (H3537)
Immobilon-Western HRP Substrate	Millipore (WBKL S0100)
L-Glutamin 200mM	Sigma (G7513)
Matrigel (without phenolred)	Corning (356237)
Neurobasal A (without Phenol red)	Gibco (12349-015)
NGS	SIGMA (G9023)
PBS	Thermo Fisher Scientific (18912014)
Penicillin/Streptomycin	Gibco (15140-122)
Protein Ladder	Thermo Scientific (26619)

Data and Software availability

Haumann, Iris (2019), "GPER1 signaling initiates migration of V-SVZ-derived cells", Mendeley Data, V1, doi: 10.17632/z6p965trkp.1

http://dx.doi.org/10.17632/z6p965trkp.1

Supplemental Figures

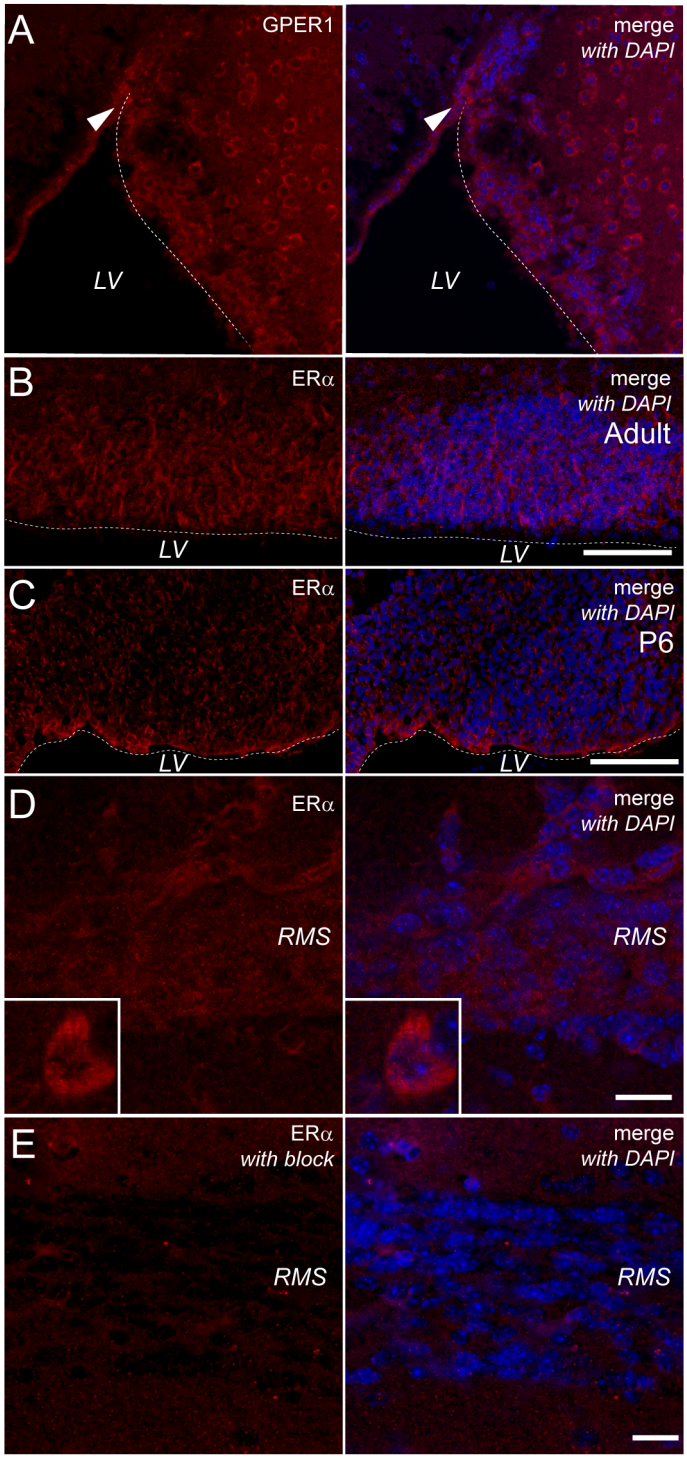

Fig. S1: ERα is expressed in the neurogenic niche and in the RMS. Related to Figure 4. GPER1 and ER alpha show a different expression pattern in DCX positive neuroblasts.

(A) Low magnification images of 7µm thick paraffin sections of an adult female mouse brain, showing GPER1 (rb) expression in the V-SVZ next to the lateral ventricle (LV). GPER1 immunoreactivity is visible in the germinal region and at the beginning of the RMS (arrowhead). (B) Confocal images of a sagittal vibratome section (of an adult female mouse brain), showing ERα expression in the V-SVZ. (C) ERα expression in the neurogenic niche is already visible at P6. Dotted lines mark the boundary between the germinal region and the lateral ventricle. (D) Confocal image showing ERα expression in the RMS of an adult female mouse (sagittal vibratome section). Note that the ERα expression can be found in the cytoplasm and/or the nucleus (higher magnification in (D)). (E) Confocal images of the RMS of an adult female mouse (sagittal vibratome section) demonstrating that

preadsorption of the ERα antibody with the immunizing peptide resulted in a disappearance of the immunofluorescence. Note that adjacent sections from (D) and (E) were processed in the same experiment. Lateral ventricle (LV); rostral migratory stream (RMS); rabbit antibody (rb). Scale bar: Scale bars: 100 µm in A and B, 20 µm in C and D.

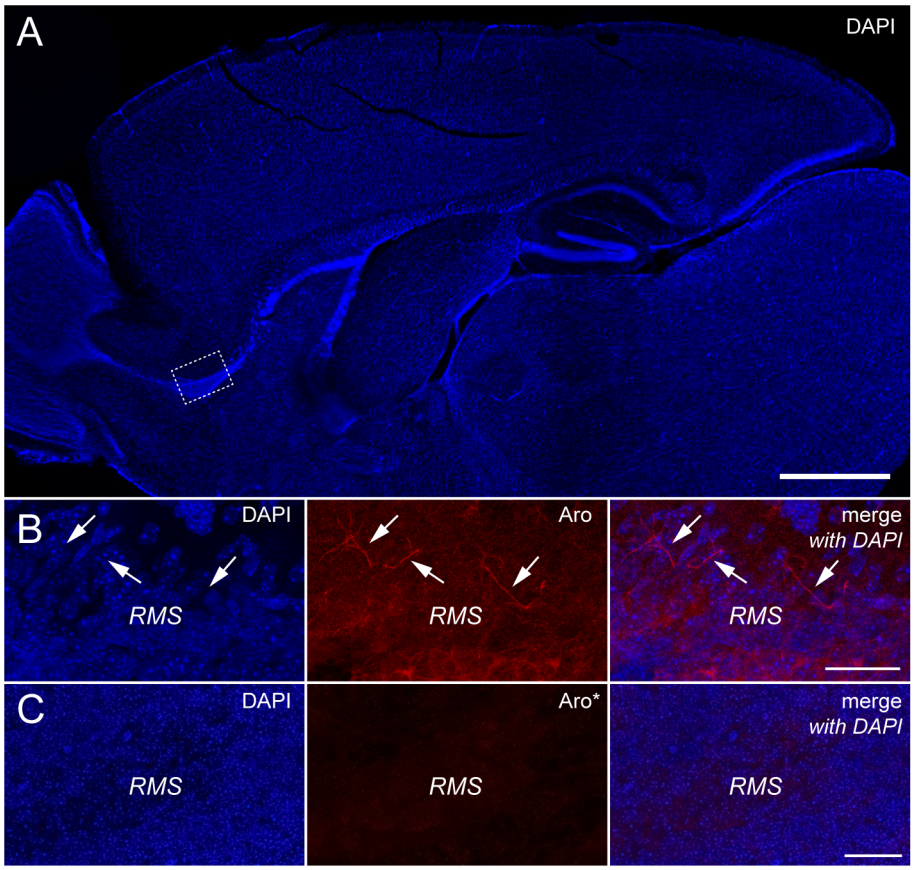

Fig.S2: Aromatase expression in the RMS. Related to Figure 5. Aromatase is expressed in the stem cell niche and in the RMS

(A) Low magnification fluorescence image with DAPI labeling, showing the RMS in a sagittal vibratome section of an adult female mouse brain. The area within the rectangular space represents the region within the RMS from which the enlarged pictures were taken. (B) Confocal images of aromatase immunoreactivity within the RMS of an adult female mouse brain. The arrows point to labeled glial cells. (C) Confocal images of the RMS of an adult female mouse (sagittal vibratome section) demonstrating that preadsorption of the aromatase antibody with the immunizing peptide resulted in a disappearance of the immunofluorescence. Note that adjacent sections from (B) and (C) were processed in the same experiment. Images were taken with the same microscope and laser settings. Rostral migratory stream (RMS); aromatase (Aro); aromatase + immunizing peptide (Aro*). Scale bars: 500 µm in A, 50 µm in B, and C.

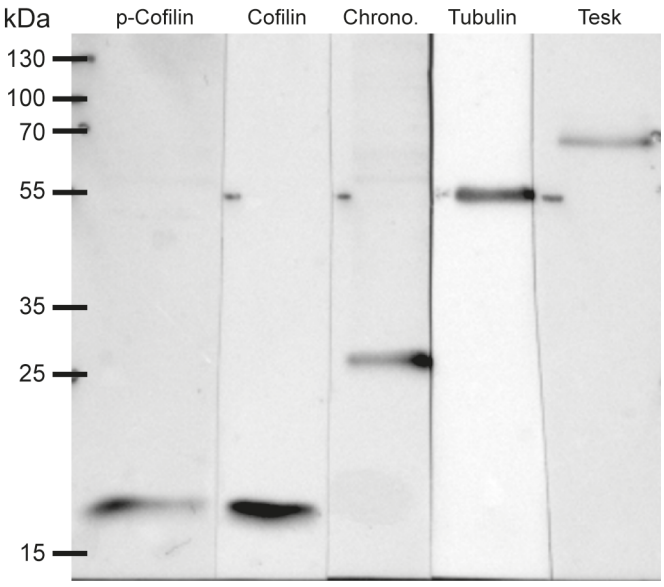

Fig. S3: Full immunoblot with all markers of molecular weight, demonstrating the specificity of the antibodies. Related to Figure 8. Treatment of explants with G15 leads to an increase in the ratio of p-cofilin/n-cofilin and influences the expression of regulators of cofilin.

Full immunoblot of V-SVZ derived tissue, showing the specificity of all antibodies used in Western Blot experiments. Every antibody shows only one specific band. kilo-Dalton (kDa); Chronophin (Chrono).